BMC Neuroscience

RESEARCH ARTICLE Open Access

Deficient hippocampal insulin signaling and augmented Tau phosphorylation is related to obesity- and age-induced peripheral insulin resistance: a study in Zucker rats

Andrea Špolcová[1], Barbora Mikulášková[1], Katarína Kršková[2], Lucia Gajdošechová[2], Štefan Zórad[2], Rafał Olszanecki[3], Maciej Suski[3], Beata Bujak-Giżycka[3], Blanka Železná[1] and Lenka Maletínská[1*]

Abstract

Background: Insulin signaling and Tau protein phosphorylation in the hippocampi of young and old obese Zucker fa/fa rats and their lean controls were assessed to determine whether obesity-induced peripheral insulin resistance and aging are risk factors for central insulin resistance and whether central insulin resistance is related to the pathologic phosphorylation of the Tau protein.

Results: Aging and obesity significantly attenuated the phosphorylation of the insulin cascade kinases Akt (protein kinase B, PKB) and GSK-3β (glycogen synthase kinase 3β) in the hippocampi of the fa/fa rats. Furthermore, the hyperphosphorylation of Tau Ser396 alone and both Tau Ser396 and Thr231 was significantly augmented by aging and obesity, respectively, in the hippocampi of these rats.

Conclusions: Both age-induced and obesity-induced peripheral insulin resistance are associated with central insulin resistance that is linked to hyperTau phosphorylation. Peripheral hyperinsulinemia, rather than hyperglycemia, appears to promote central insulin resistance and the Tau pathology in fa/fa rats.

Keywords: Zucker fa/fa rats, Insulin resistance, Obesity, GSK-3β, Tau protein

Background

Insulin resistance (IR) is a state during which a higher than normal insulin level is required for glucose homeostasis. IR occurs in the periphery and in the brain, where it has recently been linked to the hyperphosphorylation of the neuronal cytoskeleton protein Tau [1], which is symptomatic for Alzheimer's neurodegeneration. After the glucose homeostasis is disturbed, an increase in the glucose level indicates the onset of type-2 diabetes (T2D).

In several clinical studies, T2D was found to increase the risk of Alzheimer's disease (AD) [2]. In the postmortem brains of both T2D and sporadic AD patients, central resistance to insulin was documented by attenuated insulin signaling, namely via a decreased phosphorylation of the insulin cascade kinases PDK1 (3-phosphoinositide-dependent protein kinase-1), Akt (protein kinase B, PKB), and GSK-3β (glycogen synthase kinase 3β), and this effect was more pronounced in patients with both T2D and AD [3]. GSK-3β acts as both the insulin cascade kinase and the primary kinase phosphorylating Tau [4,5]. The phosphorylation of Ser9 in GSK-3β by Akt inhibits the kinase activity of GSK-3β [6,7], and the attenuated phosphorylation of Ser9 logically increases the kinase activity of GSK-3β toward Tau. Central insulin resistance is linked to a hyperphosphorylation of Tau through GSK-3β [8].

Severe hyperinsulinemia and hyperglycemia, as well as the hyperphosphorylation of Ser199/202, Thr231, and Ser396 in Tau, were found to increase progressively with age in the hippocampi of db/db mice with impaired leptin receptor signaling, a rodent model of T2D [9]. An augmented phosphorylation of Ser396 in the hippocampal Tau of db/db mice was later confirmed by another

* Correspondence: maletin@uochb.cas.cz
[1]Institute of Organic Chemistry and Biochemistry, Prague 166 10, Czech Republic
Full list of author information is available at the end of the article

research team [10]. However, in whole-brain samples of db/db mice with fully developed T2D, changes in the insulin receptors and GSK-3β phosphorylation were not found [11].

Similar to db/db mice, Zucker fatty fa/fa rats have a genetically homozygous leptin receptor mutation that results in leptin dysfunction. Zucker fa/fa rats suffer from obesity induced by hyperphagia, severe hyperlipidemia, and hyperinsulinemia, resulting in IR in the liver, muscle, and adipose tissue [12-14]. The IR in fa/fa rats is established prior to adulthood, at the age of 7 weeks [15]. Unlike db/db mice, fa/fa rats are normoglycemic or have only slightly elevated glucose levels and do not develop diabetes [12,13].

In this study, insulin signaling and Tau phosphorylation were followed in the hippocampi of 12- (young) and 33-week-old (old) obese Zucker fa/fa rats and their lean controls to verify the hypothesis that peripheral insulin resistance resulting from obesity and/or old age represents a risk factor for central insulin resistance and that such possible central IR is linked to the pathologic phosphorylation of Tau protein. In short, we aimed to determine whether IR with hyperinsulinemia but normoglycemia is associated with a risk of Tau protein pathology in the hippocampus.

Results

Metabolic parameters

In old age, both the fa/fa rats and controls developed severe obesity compared with the relevant young controls ($F_{(1,20)} = 466.52$; $p < 0.001$). The fa/fa rats also showed a significantly higher body weight than did the age-matched controls ($F_{(1,20)} = 236.30$; $p < 0.001$) (Table 1). As expected, obesity in fa/fa rats resulting from impaired leptin receptor signaling was manifested by hyperleptinemia; thus, a significant age and fa/fa genotype interaction exists ($F_{(1,20)} = 12.36$; $p < 0.01$), and a subsequent Bonferroni *post-hoc* test revealed an increase in the plasma leptin levels in young fa/fa rats compared with young controls ($p < 0.01$); this increase was more pronounced in old fa/fa rats compared with old controls ($p < 0.001$) (Table 1). Obesity was accompanied by hyperinsulinemia. There were significant effects of the fa/fa genotype ($F_{(1,20)} = 71.66$; $p < 0.001$) and age ($F_{(1,20)} = 13.94$; $p = 0.001$), as well as an age x fa/fa genotype interaction ($F_{(1,20)} = 7.99$; $p = 0.01$) with plasma insulin. Significant hyperinsulinemia in fa/fa rats was represented by extreme insulin levels that reached 12-fold ($p < 0.001$) at 12 weeks of age and 9-fold at 33 weeks of age ($p < 0.001$) in lean age-matched controls. The glucose levels in all rats were similar and did not exceed normal values (Table 1). Quantitative insulin sensitivity check index (QUICKI) was significantly decreased in both 12-week-old obese ($p < 0.05$) and 33-week-old obese rats ($p < 0.05$) compared to age-matched lean controls. Both age ($p = 0.002$) and fa/fa genotype ($p = 0.012$) were accompanied with higher and longer lasting rise in glycaemia during glucose tolerance test as revealed by general linear model for repeated measures. However, there was no interaction between these factors (Figure 1). The impairment in glucose tolerance was assessed also using parameter of 2-h glycemia during IPGTT. This impairment was observed with respect to age ($F_{(1,20)} = 19.30$; $p < 0.001$) as well as to fa/fa genotype ($F_{(1,20)} = 21.44$; $p < 0.001$). There was no detected effect of an age x fa/fa genotype interaction. The area under the curve of the glucose level during IPGTT was found to increase due only to the fa/fa genotype ($F_{(1,20)} = 5.41$; $p < 0.05$).

Dyslipidemia in young and old fa/fa rats was noticed based on the serum lipid parameters. Both total cholesterol ($F_{(1,20)} = 120.38$; $p < 0.001$) and cholesterol/HDL ratio ($F_{(1,20)} = 23.55$; $p < 0.001$) were significantly increased in fa/fa rats compared with lean rats (Table 2). Statistical analysis also revealed that age significantly affected the plasma total cholesterol ($F_{(1,20)} = 58.30$; $p < 0.001$) and cholesterol/HDL ratio ($F_{(1,20)} = 4.38$; $p < 0.05$). A significant age x fa/fa genotype interaction significantly affects the plasma total cholesterol ($F_{(1,20)} = 42.83$; $p < 0.001$) and cholesterol/HDL ratio ($F_{(1,20)} = 6.26$; $p < 0.05$). As revealed in the post-hoc test, both the plasma total cholesterol were significantly increased in young and old fa/fa rats compared with their age-matched lean controls ($p < 0.001$). An age-dependent increase in this lipid parameter was observed only in fa/fa rats ($p < 0.001$). The cholesterol/HDL ratio was increased in old fa/fa rats compared with their lean age-matched rats ($p < 0.001$) and

Table 1 Metabolic parameters of fa/fa (obese) rats and their age matched controls

Rats	Weight [g]	Leptin [ng/ml]	Insulin [ng/ml]	Glucose [mmol/l]	QUICKI
Young control	257 ± 14,17	2,02 ± 1,23	0,50 ± 0,24	6,00 ± 0,42	0,537 ± 0,071
Young fa/fa	386 ± 13,68***	36,72 ± 5,20**	6,26 ± 2,14**	6,27 ± 0,63	0,234 ± 0,008*
Old control	457 ± 21,38***	6,33 ± 1,72	1,43 ± 0,38	6,38 ± 0,43	0,274 ± 0,010
Old fa/fa	683 ± 48,31$^{\#\#\#,\ ooo}$	88,66 ± 32,71$^{\#\#\#,\ ooo}$	12,96 ± 4,50$^{\#\#\#,\ ooo}$	6,80 ± 0,51	0,216 ± 0,007^{o}

Data are mean ± SD, n = 6 animals per group. Significance is *P < 0,05, **P < 0,01 and ***P < 0,001 (*vs. young control rats, $^{\#}$vs. young fa/fa rats, ^{o}vs. old control rats) using two-way ANOVA, Bonferroni post hoc test.
Significance P<0.05, P<0.01, or P<0.001 is illustrated by one, two, or three symbols, respectively. Particular symbols are for particular groups compared.

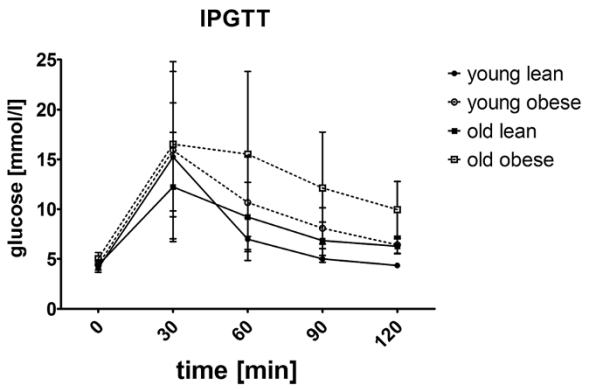

Figure 1 Graph of inraperitoneal glucose tolerance test. Before the IPGTT rats were fasted overnight. The intraperitoneal injection of 50% dextrose at dose 2 g/kg was administered and glucose was measured in the tail vein using a glucometer. Data are mean ± SD (n = 6 rats per group). Statistical analysis was calculated by two-way ANOVA, Bonferroni post hoc test.

in old fa/fa rats vs. young fa/fa rats ($p < 0.01$). In the case of plasma triglycerides levels, a significant elevation was noticed only in 33-week-old obese Zucker rats compared to lean rats of the same age.

Insulin signaling cascade in the hippocampus

Regarding the insulin cascade, a two-way ANOVA revealed a significant main effect of the fa/fa genotype ($F_{(1,20)} = 6.82$; $p < 0.05$) on insulin receptor protein expression. In Zucker fatty rats, obesity was associated with lower hippocampal insulin receptor protein levels (Figure 2). However, aging did not affect hippocampal insulin receptor protein expression ($F_{(1,20)} = 0.43$; $p < 0.52$). There was no significant interaction between age and genotype ($F_{(1,20)} = 0.78$; $p < 0.08$).

Age had a main effect on decreasing the level of PI3 kinase (PI3K) ($F_{(1,20)} = 42.03$; $p < 0.001$). The level of PI3K was also attenuated due to the fa/fa phenotype ($F_{(1,20)} = 9.84$; $p < 0.001$) (Figure 2). The two-way ANOVA revealed a significant interaction between age and genotype ($F_{(1,20)} = 17.77$; $p < 0.001$). Bonferroni's post-hoc test revealed significantly decreased levels of PI3K in young obese rats compared with young lean rats ($p < 0.001$) and in old lean rats compared with young lean rats ($p < 0.001$). No significant differences were observed between old obese and old lean rats.

As determined by the two-way ANOVA, there was significant main effect of fa/fa genotype ($F_{(1,20)} = 5.00$; $p < 0.05$) on the phosphorylation of PDK1 Ser241 in the hippocampus (Figure 2). Obesity decreased PDK1 Ser241 phosphorylation in the hippocampi of Zucker fa/fa rats. Neither a significant main effect of age nor an interaction between age and genotype was detected (Figure 2).

The two-way ANOVA revealed a significant main effect of age ($F_{(1,20)} = 27.11$; $p < 0.001$) on the phosphorylation of Akt Thr308 (Figure 2). Aging significantly attenuated the hippocampal phosphorylation of Akt Thr308 in both fa/fa and lean rats. Neither a significant effect of genotype ($F_{(1,20)} = 0.67$; $p < 0.42$) nor an interaction between age and genotype ($F_{(1,20)} = 1.80$; $p < 0.19$) was noted. Regarding the phosphorylation of Akt Ser473, significant main effects of age ($F_{(1,20)} = 31.10$; $p < 0.001$) and the fa/fa genotype ($F_{(1,20)} = 6.51$; $p < 0.05$) were observed. Both aging and obesity attenuated the phosphorylation of Akt Ser473 (Figure 2). There was no significant interaction between age and the fa/fa genotype ($F_{(1,20)} = 1.08$; $p < 0.31$).

Similarly, significant main effects of age ($F_{(1,20)} = 9.84$; $p < 0.01$) and the fa/fa genotype ($F_{(1,20)} = 12.26$; $p < 0.01$) (Figure 2) on the phosphorylation of GSK-3β Ser9 were observed. Both aging and obesity reduced the phosphorylation of GSK-3β Ser9 (Figure 2). No significant interaction between these factors was detected ($F_{(1,20)} = 0.81$; $p < 0.38$).

Table 2 Levels of lipids in blood serum of fa/fa (obese) rats and their age matched controls

Rats	Cholesterol [mmol/l]	Triglycerides [mmol/]	Cholesterol/HDL
Young control	2,25 ± 0,23	0,783 ± 0,117	1,605 ± 0,066
Young fa/fa	3,40 ± 0,41**	2,917 ± 0,703	1,988 ± 0,214
Old control	2,53 ± 0,15	0,783 ± 0,098	1,539 ± 0,067
Old fa/fa	7,08 ± 1,17$^{\#\#\#,\ ooo}$	4,000 ± 0,802^{oo}	2,736 ± 0,763$^{\#\#,\ ooo}$

Data are mean ± SD, n = 6 animals per group. Significance is *P < 0,05, **P < 0,01 and ***P < 0,001 (*vs. young control rats, $^{\#}$vs. young fa/fa rats, ^{o}vs. old control rats) using two-way ANOVA, Bonferroni post hoc test.
Significance P<0.05, P<0.01, or P<0.001 is illustrated by one, two, or three symbols, respectively. Particular symbols are for particular groups compared.

Abnormal phosphorylation of tau protein in the hippocampus

Regarding the phosphorylation of tau at Ser396 in the hippocampus, main effects of age ($F_{(1,20)} = 21.55$; $p < 0.001$) and genotype ($F_{(1,20)} = 31.16$; $p < 0.001$) were found. Both of these factors increased the phosphorylation of hippocampal tau at Ser396 (Figure 3). There was no significant interaction between age and the fa/fa genotype ($F_{(1,20)} = 1.35$; $p < 0.26$). The two-way ANOVA revealed a significant main effect of fa/fa genotype ($F_{(1,20)} = 8.86$; $p < 0.01$) on Tau Thr231 phosphorylation (Figure 3). Obesity significantly increased the phosphorylation of hippocampal Tau Thr231. Neither a significant effect of age ($F_{(1,20)} = 0.21$; $p < 0.66$) nor an interaction between age and genotype ($F_{(1,20)} = 0.05$; $p < 0.82$) was noted.

Discussion and conclusions

This study revealed attenuated insulin signaling and increased hyperphosphorylation of Tau (at Ser396 and

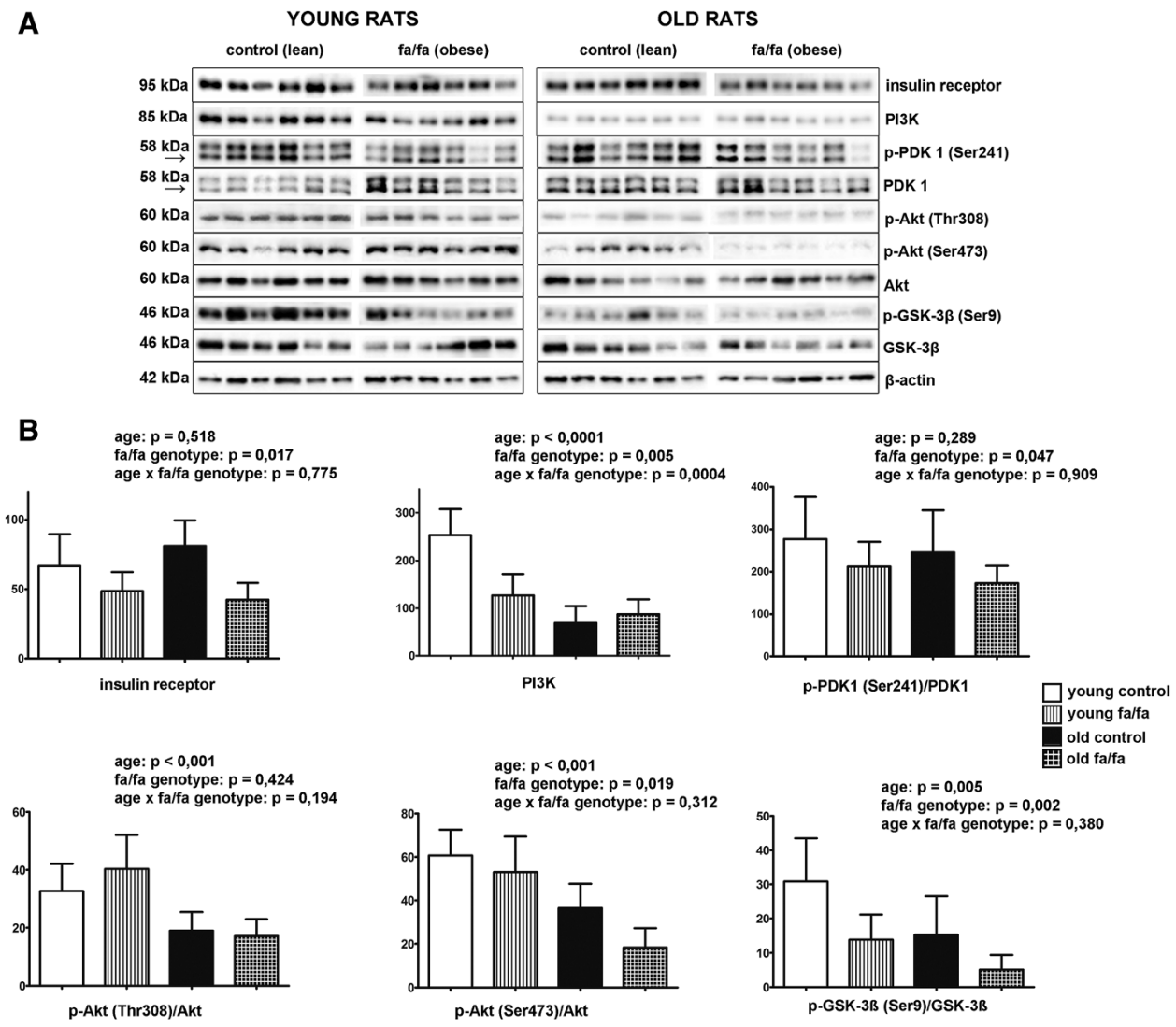

Figure 2 Insulin signaling cascade in hippocampi of fa/fa rats and their control. A Western blots of the proteins involved in insulin signaling cascade using specific antibodies (n = 6 rats per group) **B** Densitometric quantification of the western blots normalized to beta-actin: data are mean ± SD (n = 6 rats per group). Statistical analysis was calculated by two-way ANOVA, Bonferroni post hoc test.

Thr231) in the hippocampi of fa/fa rats exhibiting peripheral insulin resistance or advanced age.

Both the fa/fa rats in this study and the db/db mice in a previous work [9] exhibited impaired leptin signaling, hyperinsulinemia and blood insulin levels approximately 10-fold higher than the normal values. These data indicate that peripheral insulin resistance developed at an early age (8 and 12 weeks) in the db/db mice and the fa/fa rats, respectively. IR in the fa/fa rats was indirectly demonstrated using the QUICKI test. Dyslipidemia in the fa/fa rats could be linked to peripheral IR.

The fa/fa rats were normoglycemic even at an advanced age (33 weeks), whereas 8-week-old db/db mice had glucose levels double those of the control db + mice [9]. Glucose or glucosamine availability is considered to determine the degree of GlcNAcylation of the serines and threonines in the Tau protein that can be phosphorylated [16]. The attenuation of GlcNAcylation in favor of the augmented phosphorylation of the Tau protein has been described as a possible mechanism of Tau pathology [17-19]. On the other hand, healthy mice deprived of food for one to three days (which likely resulted in lower than normal glucose levels) exhibited reversible phosphorylation of hippocampal Tau Ser396 [20]. The fa/fa rats in the present study exhibited an obvious increase in the hyperphosphorylation of hippocampal Tau protein in the normoglycemic state. This finding supports the hypothesis that insulin ineffectiveness, rather than extreme glucose levels, is linked to Tau hyperphosphorylation.

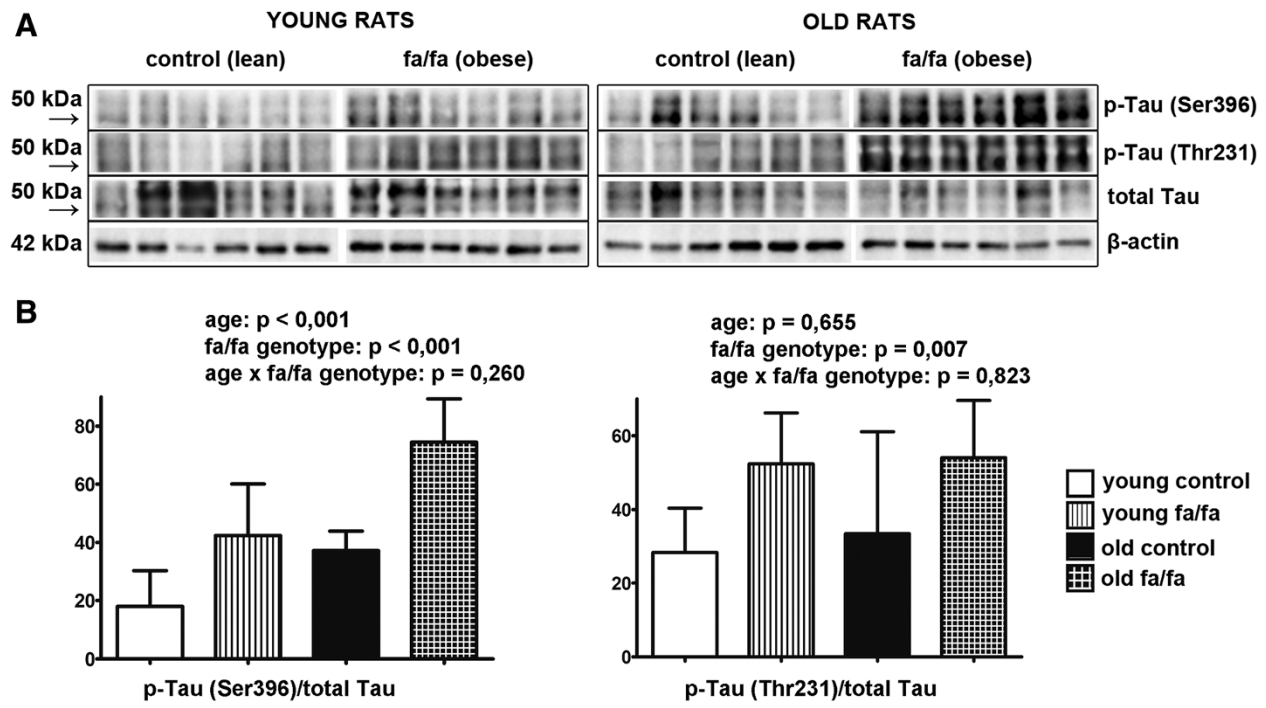

Figure 3 Hyperphosphorylation of Tau protein on different epitopes in hippocampi of fa/fa rats and their control. A Western blots of phosphorylation of Tau protein on the epitopes Ser396 and Thr231 (n = 6 rats per group) **B** Densitometric quantification of western blots normalized to β-actin: data are mean ± SD (n = 6 rats per group). Statistical analysis was calculated by two-way ANOVA, Bonferroni post hoc test.

In this study, the obese rats had significantly reduced hippocampal levels of insulin receptor and PI3 kinase protein. Statistically significantly attenuated phosphorylation of both Akt Thr308 and Ser473 was detected in old-age rats, and this effect was more pronounced in fa/fa rats. A similar trend was found for the phosphorylation of Ser9 in GSK3/β. GSK-3β, a kinase common in insulin cascading and Tau phosphorylation, is constitutively active in resting neurons, and its activity is negatively affected by Ser9 phosphorylation [6,7]. GSK-3β is the primary Tau kinase that hyperphosphorylates Tau [21-23], with Ser199, Thr231, Ser396, and Ser413 as the predominant targets [24]. Cavallini et al. [25] identified GSK-3β and also GSK-3α and MAPK13 as the most active out of 352 kinases overexpressing both Tau kinases and Tau protein [25]. Besides Akt and GSK-3β, extracellular signal-regulated kinase (ERK), is involved both in insulin signaling and Tau phosphorylation. However, there were found no differences in ERK1/2 phosphorylation between the groups in this study (not shown).

The Ser396 and Thr231 phosphorylations investigated in this study are essential in Tau protein pathology for the following reasons. Ser396 is directly phosphorylated by GSK-3β without priming (previous phosphorylation of another Ser or Thr on the Tau protein) [26]. Moreover, a positive relationship between the phosphorylation of Tau Ser396 in the cerebrospinal fluid and the severity of the disease was found in AD patients [27]. Additionally, NIRCO (neuron specific knock-out) mice without insulin receptors in brain neurons showed an increase in the phosphorylation of Tau Thr231, which resulted from the attenuated phosphorylation of Akt Ser473 and GSK-3β Ser9 [5]. Cavallini et al. [25] specified the main phosphorylation sites of Tau as Ser202, Thr231, Ser235, and Ser396/404. In addition to Ser396 and Thr231, we examined Tau phosphorylation at Ser212/214 and Ser 202 in all the groups, but the results were inconsistent.

Inefficient leptin signaling in fa/fa rats could contribute to Tau hyperphosphorylation because leptin has been reported to prevent Tau phosphorylation in neuronal cells via the activation of AMP-dependent kinase [28]. This process was later found to be stress dependent [29], making its role in Tau pathology unclear.

This study demonstrated that the phosphorylation of Ser396 and Thr231 in hippocampal Tau was related to the fa/fa obese phenotype; an interaction with the rats' age was found for Ser396 only. Analogously, in the hippocampi of db/db mice with non-functioning leptin receptors and severe IR, Tau phosphorylation at Ser 199/202, Thr231, and Ser396 was found to progress with age. Unfortunately, the previous study of

db/db mice [9] did not provide data on hippocampal insulin signaling.

In a human study [3], attenuated insulin signaling was inversely correlated with increased Tau hyperphosphorylation in the frontal cortex of T2D patients, and this correlation was more pronounced in T2D patients with AD co-morbidity. However, data on insulin, glucose, and lipid levels were not accessible because of postmortem sampling. Nevertheless, both impaired insulin signaling and Tau hyperphosphorylation in the brain were obvious in both the human study [3] and this rat study.

Peripheral IR in old-age rats appeared to result in central insulin resistance and Tau hyperprotein phosphorylation in the hippocampus. This effect was more pronounced in obese fa/fa rats, which are prone to obesity-induced IR. Based on the normoglycemic state of the IR fa/fa rats, we conclude that a pre-T2D state with IR and normoglycemia is associated with an increased risk of central pathological IR and Tau phosphorylation. The precise mechanism and the role of leptin signaling should be elucidated.

Methods

Animals

This investigation was conducted in accordance with ethical standards of the Declaration of Helsinki. This study conformed to national and international guidelines and was approved by the authors' institutional review board. All experimental procedures and animal care were carried out according to the Jagiellonian University Ethical Committee on Animal Experiments (No 75/2011).

Old (33 weeks old) and young (12 weeks old) male obese Zucker *fa/fa* rats and their age-matched lean controls (n = 6 per each group) were maintained at Jagellonian University in Krakow, Poland. Lean individuals (dominant homozygotes *Fa/Fa* or heterozygotes *Fa/fa*) served as lean controls for the obese *fa/fa* rats. The animals had free access to food and water.

The overnight-fasted rats were euthanized by decapitation. The blood glucose was measured at Synlab (Bratislava, Slovakia) using the multi-analyzer COBAS Integra 800 (Roche Diagnostics Ltd., Rotkreuz, Switzerland), and the serum leptin and insulin levels were determined using RIA kits (Millipore, USA) following the manufacturer's instructions. The measurements of the serum lipids were performed in the Laboratory Diagnostics Unit of The University Hospital in Krakow using commercially available kits (Roche Molecular Diagnostics, Pleasanton, CA, USA). The quantitative insulin sensitivity check index (QUICKI) [30] was calculated as $QUICKI = 1/[(\log(I_0) + \log(G_0)]$, where I_0 is the fasting plasma insulin level (microunits per mL), and G_0 is the fasting blood glucose level (milligrams per dL).

Intraperitoneal glucose tolerance test

All rats were subjected to an intraperitoneal glucose tolerance test (IPGTT) 2 days prior to euthanasia and after a 16-hour-long overnight fast. The rats were administered an intraperitoneal injection of 50% dextrose at a dose of 2 g/kg body weight. The blood glucose was measured using a glucometer (Accu-Chek Active, Roche Diagnostics, Germany) in the tail vein blood prior to and 30, 60, 90, and 120 min after glucose administration.

Tissue preparation for western blotting

The dissected hippocampi were homogenized in a glass microhomogenizer using lysis buffer (62.5 mM Tris–HCl buffer with pH 6.8, 1% deoxycholate, 1% Triton X-100, 50 mM NaF, 1 mM Na_3VO_4, and Complete Protease Inhibitor (Roche, Switzerland). The lysates were sonicated for 10 min and boiled for 10 minutes. The samples for electrophoresis at 1 μg/μl were diluted with a Laemmli sample buffer containing 50 mM NaF and 1 mM Na_3VO_4.

Antibodies

The following primary antibodies were used: insulin receptor rabbit mAb, PI3 kinase rabbit Ab, phospho-PDK1 (Ser241) rabbit mAb, PDK1 rabbit mAb, phospho-Akt (Thr308) rabbit mAb, phospho-Akt (Ser473) rabbit mAb, Akt rabbit mAb, phospho-GSK-3β (Ser9) rabbit mAb, and GSK-3 β rabbit mAb (all from Cell Signaling Technology, Beverly, MA, USA); phosphoTau (Ser396) rabbit mAb and phosphoTau (Thr231) rabbit mAb (clone PHF13.6 and PHF-6, respectively, both from Invitrogen, NY, USA); CTer mouse mAb for total Tau protein (gift from Dr. M.-C. Galas, Inserm U837, Lille, France); and beta-actin mouse mAb (from Sigma Aldrich). The following secondary antibodies were used: anti-mouse IgG HRP-linked antibody and anti-rabbit IgG HRP-linked antibody (both from Cell Signaling Technology, Beverly, MA, USA).

Western blotting

Samples of 2–15 μg total protein were subjected to 4/10% SDS-PAGE and transferred onto nitrocellulose (BIO-RAD) or polyvinylidene difluoride (Sigma Aldrich) membranes. The blots were blocked in 5% non-fat milk or 3% BSA in a TBS/Tween buffer (20 mM Tris, 136 mM NaCl, 0.1% Tween-20) with 50 mM NaF and 1 mM Na_3VO_4, incubated with the appropriate primary antibody, then incubated with the HRP-linked secondary antibody and developed using the SuperSignal West Femto maximum sensitivity substrate (Pierce, Rockford, IL, USA) following the manufacturer's instructions. The bands were visualized using the ChemiDoc™ System (BIO-RAD, Hercules, CA, USA) and were quantified using Image Lab Software (BIO-RAD, Hercules, CA, USA). The band intensities were normalized using actin as an internal loading compound,

and the ratios of the intensity of the band with the phosphorylated protein and the intensity of the band with the total level of protein were calculated.

Statistical analysis

The data were analyzed using IBM SPSS 19 Software and are presented as the means ± SD. The data were tested for normality by Shapiro-Wilk test. Normally distributed data were analysed by two-way analysis of variance with interaction with factors of age and fa/fa genotype. Non-normally distributed data were subjected to natural logarithm transformation followed by two-way ANOVA (insulin). Data without normal distribution despite the use of above mentioned transformation were analysed by non-parametric Kruskal-Wallis test (QUICKI, triglycerides). General Linear Model for Repeated Measures was used to evaluate differences in glycaemia during IPGTT. Total area under the curve (AUC) was calculated to describe increment of plasma glucose levels after exogenous glucose load. The overall level of statistical significance was $p < 0.05$.

Competing interests

The authors declare that there is no competing interest that could be perceived as prejudicing the impartiality of the research reported.

Authors' contributions

AS performed partly sampling and western blots and partly drafted the manuscript, BB performed western blots, KK performed sampling and partly analyses of the blood samples, LG performed sampling, analyses of the blood samples and partly drafted the manuscript, SZ was partly responsible for conception and design of the study, RO was partly responsible for the conception and design of the study. BB-G and MS were partly responsible for analyses of the blood samples, BZ and LM partly drafted the manuscript, LM was corresponding author. All authors read and approved the final manuscript.

Acknowledgements

This project was supported by GACR P303/12/0576 and RVO:61388963 (Czech Rep.), VEGA 2/0089/11 and APVV 0028–10 (Slovakia) and 2011/01 M/NZ04/03752 (Poland). The authors are indebted to Dr. M.-C. Galas, Inserm U837, Lille, France for providing the total Tau protein antibody.

Author details

[1]Institute of Organic Chemistry and Biochemistry, Prague 166 10, Czech Republic. [2]Institute of Experimental Endocrinology, Bratislava 833 06, Slovakia. [3]Jagiellonian University Medical College, Chair of Pharmacology, Krakow 310 08, Poland.

Received: 17 September 2013 Accepted: 18 September 2014
Published: 25 September 2014

References

1. Deng Y, Li B, Liu Y, Iqbal K, Grundke-Iqbal I, Gong CX: **Dysregulation of insulin signaling, glucose transporters, O-GlcNAcylation, and phosphorylation of tau and neurofilaments in the brain: Implication for Alzheimer's disease.** *Am J Pathol* 2009, **175**(5):2089–2098.
2. Kopf D, Frölich L: **Risk of incident Alzheimer's disease in diabetic patients: a systematic review of prospective trials.** *J Alzheimers Dis* 2009, **16**(4):677–685.
3. Liu Y, Liu F, Grundke-Iqbal I, Iqbal K, Gong CX: **Deficient brain insulin signalling pathway in Alzheimer's disease and diabetes.** *J Pathol* 2011, **225**(1):54–62.
4. Hong M, Lee VM: **Insulin and insulin-like growth factor-1 regulate tau phosphorylation in cultured human neurons.** *J Biol Chem* 1997, **272**(31):19547–19553.
5. Schubert M, Gautam D, Surjo D, Ueki K, Baudler S, Schubert D, Kondo T, Alber J, Galldiks N, Küstermann E, Arndt S, Jacobs AH, Krone W, Kahn CR, Brüning JC: **Role for neuronal insulin resistance in neurodegenerative diseases.** *Proc Natl Acad Sci U S A* 2004, **101**(9):3100–3105. Epub 2004 Feb 23.
6. Sutherland C, Leighton IA, Cohen P: **Inactivation of glycogen synthase kinase-3 beta by phosphorylation: new kinase connections in insulin and growth-factor signalling.** *Biochem J* 1993, **296**(Pt 1):15–19.
7. Cross DA, Alessi DR, Cohen P, Andjelkovich M, Hemmings BA: **Inhibition of glycogen synthase kinase-3 by insulin mediated by protein kinase B.** *Nature* 1995, **378**(6559):785–789.
8. Takashima A: **GSK-3 is essential in the pathogenesis of Alzheimer's disease.** *J Alzheimers Dis* 2006, **9**(3 Suppl):309–317.
9. Kim B, Backus C, Oh S, Hayes JM, Feldman EL: **Increased tau phosphorylation and cleavage in mouse models of type 1 and type 2 diabetes.** *Endocrinology* 2009, **150**(12):5294–5301.
10. Li J, Deng J, Sheng W, Zuo Z: **Metformin attenuates Alzheimer's disease-like neuropathology in obese, leptin-resistant mice.** *Pharmacol Biochem Behav* 2012, **101**(4):564–574.
11. Jolivalt CG, Lee CA, Beiswenger KK, Smith JL, Orlov M, Torrance MA, Masliah E: **Defective insulin signaling pathway and increased glycogen synthase kinase-3 activity in the brain of diabetic mice: parallels with Alzheimer's disease and correction by insulin.** *J Neurosci Res* 2008, **86**(15):3265–3274.
12. www.criver.com.
13. www.harlan.com.
14. Shiota M, Printz RL: **Diabetes in Zucker diabetic fatty rat.** *Methods Mol Biol* 2012, **933**:103–123.
15. Di Nardo F, Burattini R, Cogo CE, Faelli E, Ruggeri P: **Age-related analysis of insulin resistance, body weight and arterial pressure in the Zucker fatty rat.** *Exp Physiol* 2009, **94**(1):162–168.
16. Walgren JL, Vincent TS, Schey KL, Buse MG: **High glucose and insulin promote O-GlcNAc modification of proteins, including alpha-tubulin.** *Am J Physiol Endocrinol Metab* 2003, **284**(2):E424–E434.
17. Dias WB, Hart GW: **O-GlcNAc modification in diabetes and Alzheimer's disease.** *Mol Biosyst* 2007, **3**(11):766–772.
18. Deng Y, Li B, Liu F, Iqbal K, Grundke-Iqbal I, Brandt R, Gong CX: **Regulation between O-GlcNAcylation and phosphorylation of neurofilament-M and their dysregulation in Alzheimer disease.** *FASEB J* 2008, **22**(1):138–145.
19. Lefebvre T, Dehennaut V, Guinez C, Olivier S, Drougat L, Mir AM, Mortuaire M, Vercoutter-Edouart AS, Michalski JC: **Dysregulation of the nutrient/stress sensor O-GlcNAcylation is involved in the etiology of cardiovascular disorders, type-2 diabetes and Alzheimer's disease.** *Biochim Biophys Acta* 2010, **1800**(2):67–79.
20. Yanagisawa M, Planel E, Ishiguro K, Fujita SC: **Starvation induces tau hyperphosphorylation in mouse brain: implications for Alzheimer's disease.** *FEBS Lett* 1999, **461**(3):329–333.
21. Ishiguro K, Omori A, Takamatsu M, Sato K, Arioka M, Uchida T, Imahori K: **Phosphorylation sites on tau by tau protein kinase I, a bovine derived kinase generating an epitope of paired helical filaments.** *Neurosci Lett* 1992, **148**(1–2):202–206.
22. Yamaguchi H, Ishiguro K, Uchida T, Takashima A, Lemere CA, Imahori K: **Preferential labeling of Alzheimer neurofibrillary tangles with antisera for tau protein kinase (TPK) I/glycogen synthase kinase-3 beta and cyclin-dependent kinase 5, a component of TPK II.** *Acta Neuropathologica* 1996, **92**(3):232–241.
23. Hooper C, Killick R, Lovestone S: **The GSK3 hypothesis of Alzheimer's disease.** *J Neurochem* 2008, **104**(6):1433–1439.
24. Michel G, Mercken M, Murayama M, Noguchi K, Ishiguro K, Imahori K, Takashima A: **Characterization of tau phosphorylation in glycogen synthase kinase-3beta and cyclin dependent kinase-5 activator (p23) transfected cells.** *Biochim Biophys Acta* 1998, **1380**(2):177–182.
25. Cavallini A, Brewerton S, Bell A, Sargent S, Glover S, Hardy C, Moore R, Calley J, Ramachandran D, Poidinger M, Karran E, Davies P, Hutton M, Szekeres P, Bose S: **An unbiased approach to identifying tau kinases that phosphorylate tau at sites associated with Alzheimer disease.** *J Biol Chem* 2013, **288**(32):23331–23347.
26. Leroy A, Landrieu I, Huvent I, Legrand D, Codeville B, Wieruszeski JM, Lippens G: **Spectroscopic studies of GSK3{beta} phosphorylation of the**

neuronal tau protein and its interaction with the N-terminal domain of apolipoprotein E. *J Biol Chem* 2010, **285**(43):33435–33444.
27. Hu YY, He SS, Wang X, Duan QH, Grundke-Iqbal I, Iqbal K, Wang J: **Levels of nonphosphorylated and phosphorylated tau in cerebrospinal fluid of Alzheimer's disease patients: an ultrasensitive bienzyme-substrate-recycle enzyme-linked immunosorbent assay.** *Am J Pathol* 2002, **160**(4):1269–1278.
28. Greco SJ, Sarkar S, Johnston JM, Zhu X, Su B, Casadesus G, Ashford JW, Smith MA, Tezapsidis N: **Leptin reduces Alzheimer's disease-related tau phosphorylation in neuronal cells.** *Biochem Biophys Res Commun* 2008, **376**(3):536–541.
29. Salminen A, Kaarniranta K, Haapasalo A, Soininen H, Hiltunen M: **AMP-activated protein kinase: a potential player in Alzheimer's disease.** *J Neurochem* 2011, **118**(4):460–474.
30. Katz A, Nambi SS, Mather K, Baron AD, Follmann DA, Sullivan G, Quon MJ: **Quantitative insulin sensitivity check index: a simple, accurate method for assessing insulin sensitivity in humans.** *J Clin Endocrinol Metab* 2000, **85**(7):2402–2410.

doi:10.1186/1471-2202-15-111
Cite this article as: Špolcová *et al.*: Deficient hippocampal insulin signaling and augmented Tau phosphorylation is related to obesity- and age-induced peripheral insulin resistance: a study in Zucker rats. *BMC Neuroscience* 2014 **15**:111.

International Journal of Obesity (2015), 1–8

www.nature.com/ijo

ORIGINAL ARTICLE

Novel lipidized analogs of prolactin-releasing peptide have prolonged half-lives and exert anti-obesity effects after peripheral administration

L Maletínská[1], V Nagelová[1], A Tichá[1], J Zemenová[1,2], Z Pirník[1,3,4], M Holubová[1], A Špolcová[1], B Mikulášková[1,5], M Blechová[1], D Sýkora[2], Z Lacinová[6], M Haluzík[6], B Železná[1] and J Kuneš[1,5]

OBJECTIVES: Obesity is a frequent metabolic disorder but an effective therapy is still scarce. Anorexigenic neuropeptides produced and acting in the brain have the potential to decrease food intake and ameliorate obesity but are ineffective after peripheral application. We have designed lipidized analogs of prolactin-releasing peptide (PrRP), which is involved in energy balance regulation as demonstrated by obesity phenotypes of both PrRP- and PrRP-receptor-knockout mice.

RESULTS: Lipidized PrRP analogs showed binding affinity and signaling in PrRP receptor-expressing cells similar to natural PrRP. Moreover, these analogs showed high binding affinity also to anorexigenic neuropeptide FF-2 receptor. Peripheral administration of myristoylated and palmitoylated PrRP analogs to fasted mice induced strong and long-lasting anorexigenic effects and neuronal activation in the brain areas involved in food intake regulation. Two-week-long subcutaneous administration of palmitoylated PrRP31 and myristoylated PrRP20 lowered food intake, body weight and improved metabolic parameters, and attenuated lipogenesis in mice with diet-induced obesity.

CONCLUSIONS: Our data suggest that the lipidization of PrRP enhances stability and mediates its effect in central nervous system. Strong anorexigenic and body-weight-reducing effects make lipidized PrRP an attractive candidate for anti-obesity treatment.

International Journal of Obesity advance online publication, 14 April 2015; doi:10.1038/ijo.2015.28

INTRODUCTION

Prolactin-releasing peptide (PrRP) was originally discovered as an endogenous ligand of an orphan G-protein-coupled receptor.[1] PrRP and its receptor named GPR10 were detected in several hypothalamic nuclei,[2] suggesting an involvement of PrRP in the control of food intake and body weight.[3] PrRP was also found to have high affinity to the neuropeptide FF-2 (NPFF2) receptor, resulting in anorexigenic effect.[4] The endogenous ligand of NPFF2 receptor, NPFF, also has hyperalgesic and anti-morphine analgesic properties (for reviews, see[5,6]).

The suggestion that PrRP may act as a homeostatic regulator of food intake was supported by the finding that PrRP messenger RNA (mRNA) expression was reduced in situations of negative energy balance similarly to other anorexigenic peptides such as α-melanocyte stimulating hormone or cocaine- and amphetamine-regulated transcript peptide.[3] The intracerebroventricular administration of PrRP inhibited food intake and body weight gain in rats but did not cause conditioned taste aversion.[7] Furthermore, Fos immunoreactivity was enhanced after PrRP administration in the brain areas associated with food intake regulation.[7]

Finally, PrRP-receptor-knockout mice had significantly higher body weight at 15 weeks of age compared with wild-type mice, and this late-onset obesity was much more pronounced in female mice, which also exhibited a significant decrease in energy expenditure.[8] Similarly, PrRP-deficient mice displayed late-onset obesity, increased food intake and attenuated responses to the anorexigenic signals cholecystokinin and leptin.[9]

Taken together, these findings suggest that PrRP and other anorexigenic neuropeptides involved in food intake regulation[10,11] may have a potential in the development of future anti-obesity agents. Nevertheless, because these peptides normally regulate food intake directly in the hypothalamus, their anorexigenic potential after peripheral administration is hampered by their inability to cross the blood-brain barrier (BBB) and to reach the target brain receptors.

For the design of peptide drugs, the lipidization of peptides, that is, the attachment of fatty-acid chain to peptides through ester or amide bond is advantageous. Such modification results in an increased stability and half-life of the peptide, and it is possible that these modifications allow peptide to cross the BBB after a peripheral administration (reviewed by[12–14]). Myristoylation or palmitoylation through an amide bond on a Lys has been employed in the insulin analog detemir[15] or glucagon-like peptide 1 analog liraglutide.[16] Both of these peripherally acting lipopeptide drugs show strongly prolonged half-lives and slower biodegradation. Central effects of detemir and liraglutide have been described suggesting that the attachment of fatty acid may also enable these peptides to cross the BBB.[17]

PrRP seems to be a suitable candidate for lipidization because of its linear, one-chain peptide structure. Two biologically active

[1]Antiobesity Peptides, Institute of Organic Chemistry and Biochemistry, AS CR, Prague, Czech Republic; [2]Department of Analytical Chemistry, University of Chemistry and Technology, Prague, Czech Republic; [3]Laboratory of Functional Neuromorphology, Institute of Experimental Endocrinology, SAS, Bratislava, Slovak Republic; [4]Department of Human and Clinical Pharmacology, University of Veterinary Medicine, Košice, Slovak Republic; [5]Institute of Physiology, AS CR, Prague, Czech Republic and [6]Third Department of Medicine, Charles University in Prague, Prague, Czech Republic. Correspondence: Dr L Maletínská, Antiobesity Peptides, Institute of Organic Chemistry and Biochemistry, AS CR, Flemingovo nam. 2, Prague 6 166 10, Czech Republic.
E-mail: maletin@uochb.cas.cz
Received 29 August 2014; revised 10 February 2015; accepted 19 February 2015; accepted article preview online 16 March 2015

isoforms of PrRP, with either 31 (PrRP31) or 20 (PrRP20) amino acids contain a C-terminal Arg-Phe-amide sequence that is critical for the preservation of biological activity of PrRP.[18–20]

The aim of this study was to achieve the direct central anorexigenic activity of PrRP via its peripheral route of administration employing the lipidization of its N terminus. We tested a series of PrRP analogs modified with fatty acids of various lengths both *in vitro* and *in vivo*. The data showed that myristoylated PrRP20 and palmitoylated PrRP31 retained the biological activity of PrRP while significantly decreasing food intake and body weight and improving metabolic parameters upon peripheral administration in mice with diet-induced obesity. Thus, the lipidization of neuropeptides involved in food intake regulation might serve as a tool to retain their ability to act centrally after peripheral administration.

MATERIALS AND METHODS

Peptide synthesis and iodination

Rat PrRP analogs (for structure see Table 1), human PrRP31 (SRTHRHSMEIRTPDINPAWYASRGIRPVGRF-NH_2), scrambled peptides (SHQ RPADTHWYPRGNIeFPTIGRITARNGEVSR-NH_2 and (N-myr)SHQRPADTHWYP RGNIeFPTIGRITARNGEVSR-NH_2) and a stable analog of NPFF, 1DMe (D-YL(N-Me)FQPQRF-NH_2) were synthesized and purified as described previously.[21] Lipidization of PrRP analogs was performed as shown in[22] on fully protected peptide on resine as a last step. The purity and identity of all peptides were determined by analytical high-performance liquid chromatography and by using a Q-TOF micro MS technique (Waters, Milford, MA, USA).

Rat or human PrRP31 and 1DMe were iodinated at Tyr^{20} and D-Tyr^1, respectively, with $Na^{125}I$ (Izotop, Budapest, Hungary) as described previously.[22]

Binding to intact plated cells and cell membranes

Rat pituitary RC-4B/C cells obtained from ATCC (Manassas, VA, USA) were grown as described previously[24] and Chinese hamster ovarian (CHO)-K1 cells with GPR10 receptor (Perkin Elmer, Waltham, MA, USA) according to manufacturer's instructions. Saturation and competitive binding experiments were performed according to Motulsky and Neubig.[25] RC-4B/C or CHO-K1 cells were incubated with 0.5–5 nM ^{125}I-rPrRP31 or ^{125}I-hPrRP31, respectively, in saturation experiments or with 0.1 nM ^{125}I-rPrRP31 or with 0.03 nM ^{125}I-hPrRP31, respectively, and 10^{-11}–10^{-5}M non-radioactive ligands in competitive binding experiments. Experiments were performed on plates incubated for 60 min at 25 °C. Non-specific binding was determined using 10^{-5}M PrRP31. Binding assays on human NPFF2 receptor membranes obtained from Perkin Elmer were performed as described in.[24]

Detection of MAPK/ERK1/2 phosphorylation by western blotting

CHO-K1 cells were incubated with PrRP31, PrRP20, palm-PrRP31 or myr-PrRP20 with final concentrations from 10^{-7}–10^{-12}M for 5 min at 37 °C. The cells were lysed and western blots carried out as described in.[26]

Stability of PrRP analogs *in vitro*

Rat plasma fortified with a solution of the studied compound at a concentration of 3×10^{-6}M was incubated at 37 °C. The times of sampling were 0–24 h for PrRP31 and PrRP20 and 0–96 h for palm-PrRP31 and myr-PrRP20. Samples were collected in triplicates and stored at − 20 °C. The PrRP(1–31) EIA high-sensitivity kit (Peninsula Laboratories, San Carlos, CA, USA) was used according to the manufacturer's instructions.

Pharmacokinetics *in vivo* in mice

All animal experiments followed the ethical guidelines for animal experiments and the Act of the Czech Republic Nr. 246/1992 and were approved by the Committee for Experiments with Laboratory Animals of the ASCR.

The measurement of *in vivo* pharmacokinetics was performed as previously described.[23] C57BL/6 male mice were injected subcutaneously (SC) with PrRP31, PrRP20, palm-PrRP31 or myr-PrRP20 (dissolved in saline; Sal) at a dose of 5 mg kg^{-1} ($n = 3$), blood plasma collected and peptides determined by PrRP(1–31) EIA high-sensitivity kit.

Acute food intake in lean mice

Male C57BL/6 mice from Charles Rivers Laboratories (Sulzfeld, Germany) were housed at a temperature of 23 °C and a daily cycle of 12 h light and dark (lights on at 6:00). The mice were given *ad libitum* water and standard chow diet (St-1, Mlýn Kocanda, Jesenice, Czech Republic). Following schedules were used for food intake monitoring after single administration of peptides: (a) on the day of the food intake experiment, overnight (17 h) fasted mice were injected SC with Sal or PrRP analogs at doses of 0.1–5 mg kg^{-1} (all dissolved in Sal) ($n = 6$–8). Fifteen minutes after injection, the mice were given weighed food pellets. The pellets were weighed every 30 min for at least 6 h. (b) Freely fed mice were injected SC with Sal or PrRP analogs at a dose of 5 mg kg^{-1} (all dissolved in Sal) ($n = 6$) 30 min before lights out. Food intake was monitored every 10 min for at least 14 h using automatic food intake monitoring system (Development Workshops of IOCB, Prague, Czech Republic).

Fos immunohistochemistry

For c-Fos immunohistochemical processing, overnight-fasted male mice with the free access to water ($n = 4$) were SC injected with Sal or PrRP31, oct-PrRP31, myr-PrRP20 or palm-PrRP31 at a dose of 5 mg kg^{-1}. Ninety minutes after injection, the mice were deeply anesthetized with sodium pentobarbital (50 mg kg^{-1}, intraperitoneally) and perfused transcardially, the brains were treated and c-Fos immunoreactivity determined as described in.[27,28]

Table 1. Structures and binding affinities of PrRP analogs

Analog	*Sequence*	*Human GPR10. ^{125}I-human PrRP31 binding K_i (nM)*	*Human NPFF2.^{125}I-1DMe binding K_i (nM)*	*RC-4B/C cells. ^{125}I-rat PrRP31 binding K_i (nM)*
PrRP31	SRAHQHSMETRTPDINPAWYTGRGIRPVGRF-NH_2	3.91 ± 0.21	42.21 ± 6.76	2.38 ± 0.11
oct-PrRP31	(N-oct)SRAHQHS Nle ETRTPDINPAWYTGRGIRPVGRF-NH_2	1.49 ± 0.07	24.82 ± 13.2	0.98 ± 0.22
dec-PrRP31	(N-dec)SRAHQHS Nle ETRTPDINPAWYTGRGIRPVGRF-NH_2	1.42 ± 0.55	14.73 ± 3.10	0.68 ± 0.12
dodec-PrRP31	(N-dodec)SRAHQHS Nle ETRTPDINPAWYTGRGIRPVGRF-NH_2	1.15 ± 0.35	14.28 ± 6.40	0.38 ± 0.14
myr-PrRP31	(N-myr)SRAHQHS Nle ETRTPDINPAWYTGRGIRPVGRF-NH_2	0.69 ± 0.09	1.59 ± 0.32	0.69 ± 0.09
palm-PrRP31	(N-palm)SRAHQHS Nle ETRTPDINPAWYTGRGIRPVGRF-NH_2	2.94 ± 0.33	0.69 ± 0.36	0.51 ± 0.15
stear-PrRP31	(N-stear)SRAHQHS Nle ETRTPDINPAWYTGRGIRPVGRF-NH_2	5.24 ± 0.57	15.92 ± 14.43	0.93 ± 0.08
PrRP20	TPDINPAWYTGRGIRPVGRF-NH_2	4.4 ± 0.77	21.80 ± 9.91	2.23 ± 0.19
oct-PrRP20	(N-oct)TPDINPAWYTGRGIRPVGRF-NH_2	1.88 ± 0.31	48.13 ± 13.19	0.91 ± 0.23
dec-PrRP20	(N-dec)TPDINPAWYTGRGIRPVGRF-NH_2	2.94 ± 0.47	3.60 ± 2.57	0.41 ± 0.01
dodec-PrRP20	(N-dodec)TPDINPAWYTGRGIRPVGRF-NH_2	2.34 ± 0.25	9.97 ± 3.48	0.58 ± 0.22
myr-PrRP20	(N-myr)TPDINPAWYTGRGIRPVGRF-NH_2	4.21 ± 0.24	8.23 ± 1.97	1.02 ± 0.20

Abbreviations: dec, decanoyl; dodec, dodecanoyl; myr, myristoyl; Nle, norleucine; oct, octanoyl; palm, palmitoyl; stear, stearoyl. The means ± s.e.m. of at least three separate experiments are shown. In competitive binding, K_i was calculated using the Cheng–Prusoff equation. The concentration of the radioligand was 0.1 nM or 0.03 nM, and the K_d that was calculated from saturation experiments was 4.21 ± 0.66 nM for RC-4B/C[23] or 0.95 ± 0.20 nM for GPR10 receptor in CHO cells, respectively. K_d for NPFF2 receptor in CHO cells was 0.72 ± 0.12 nM.

Behavioral tests in mice

Locomotor activity and analgesia were measured in free-fed mice using the VideoMot system (TSE Systems, Bad Homburg, Germany) after the SC injection of Sal, PrRP31, oct-PrRP31, palm-PrRP31 and myr-PrRP20 at a dose of 5 mg kg^{-1} ($n = 5$) as described previously.[28,29]

The elevated plus maze (TSE Systems) test was used to measure anxiety/fear behavior. The total time spent in open and closed arms was measured.

Determination of prolactin release in rats and mice

Male Wistar rats (250–300 g, Harlan Laboratories, Correzzana, Italy, $n = 3$) were injected intravenously into the jugular vein with Sal, thyrotropin-releasing hormone (10 μg kg^{-1}) or palm-PrRP31 (0.5 mg kg^{-1}), or SC with Sal or palm-PrRP31 (5 mg kg^{-1}). Blood was collected from carotid artery before injections and 5 and 10 min after injections. Male C57BL/6 mice were injected SC with Sal, myr-PrRP20 or palm-PrRP31 (5 mg kg^{-1}). Blood was collected by decapitation 10 min after injection. Prolactin (PRL) in rat or mouse serum was determined with a radioimmunoassay assay kit (Izotop).

Effect of 14-day administration of palm-PrRP31 and myr-PrRP20 on food intake and metabolic parameters in mice with high-fat diet-induced obesity

From 8 weeks of age, C57BL/6 mice were supplied with a high-fat (HF) diet for 12 weeks to induce obesity. The energy content of the HF diet was 5.3 kcal g^{-1}, with 13%, 60% and 27% of the calories derived from protein, fat and carbohydrate, respectively.[30] Food intake and body weight were monitored weekly from 9 to 18 weeks of age. Mice resistant to the HF diet were withdrawn from the experiment (~10% of mice).

At the age of 19 weeks, the mice were divided into groups of 10 animals and placed into the separate cages with free access to HF diet and water. Three groups were injected SC either with Sal or with palm-PrRP31 or myr-PrRP20 at a dose of 5 mg kg^{-1} twice a day. The fourth group served as pair-fed controls to the animals treated with palm-PrRP31, and was given food amount consumed by palm-PrRP31 treated mice the previous day. The amount of the HF diet consumed and the weight of the mice were monitored daily.

At the end of the experiment, overnight-fasted mice were killed by decapitation starting at 8:00 a.m. The trunk blood was collected, and the plasma was separated and stored at −20 °C. The intraperitoneal adipose tissue (IPAT), subcutaneous adipose tissue (SCAT), the perirenal adipose tissue, the brown adipose tissue and the liver of all mice were dissected, weighed and stored at − 70 °C.

Determination of hormonal and biochemical parameters

The plasma insulin concentrations were measured with radioimmunoassay assays (Linco Research, St Charles, MI, USA), leptin concentrations were determined with enzyme-linked immuno assay (Millipore, St Charles, MI, USA), corticosterone levels were determined with radioimmunoassay assay kit (Izotop) and adrenocorticotropic hormone with enzyme-linked immuno assay (Peninsula Laboratories). The plasma glucose levels were measured using a Glucocard glucometer (Arkray, Kyoto, Japan). The plasma triglyceride levels were measured by quantitative enzymatic reactions (Sigma, St Louis, MO, USA).

Determination of mRNA expression

Samples of adipose tissue (IPAT, SCAT) and liver were processed as described in.[31] Determination of the mRNA expression of genes of interest (ACACA and FASN in liver, IPAT and SCAT; lipoprotein lipase, adiponectin and leptin in IPAT and SCAT, FABP-4 in liver, UCP-1 in brown adipose tissue) was performed using an ABI PRISM 7500 instrument (Applied Biosystems, Foster City, CA, USA). The expression of beta-2-microglobulin was used to compensate for variations in input RNA amounts and the efficiency of reverse transcription. (ACACA—acetyl-CoA carboxylase 1, FASN—fatty-acid synthase, LPL—lipoprotein lipase, SREBP—sterol regulatory element-binding protein, FABP-4—fatty-acid binding protein 4, UCP-1—uncoupling protein-1).

Analysis of binding data and statistics

The saturation binding curves were plotted using GraphPad software (San Diego, CA, USA) comparing the best fit for single binding site models (K_d, B_{max} and IC_{50} values were obtained from nonlinear regression analysis). Inhibition constants (K_i) were calculated from the IC_{50} values using the Cheng–Prusoff equation.[32]

The data are presented as the means ± s.e.m. for the number of animals indicated in the figures and tables. The data were analyzed using one-way analysis of variance followed by the Dunnett's *post hoc* test or a *t*-test, as stated in the figure and table legends, using the GraphPad Software.

RESULTS

Lipidized analogs of PrRP20 and PrRP31 are agonists of the PrRP receptor GPR10 and have high affinity to both GPR10 and NPFF2 receptors

The peptide sequences were assembled on a solid support as described in the Materials and Methods. The purity of all peptides was higher than 95%. The structures of the PrRP analogs used in this study are shown in Table 1. PrRP20 and PrRP31 were lipidized at the N terminus with fatty acids of different lengths. Lipidized PrRP31 analogs were modified with norleucine in position 8 to avoid oxidation of the original methionine. Analogously to a similar modification of the cocaine- and amphetamine-regulated transcript peptide,[33] the change of methionine for norleucine did not affect the biological activity of PrRP31.

All native and lipidized analogs of PrRP31 and PrRP20 competed with human ^{125}I-PrRP31 for binding to CHO cells overexpressing the human PrRP receptor GPR10 with K_i values in a nanomolar range, as shown in Table 1. Scrambled peptide based on PrRP20 and its myristoylated analog (structures in the Methods) were bound to GPR10 receptor with a negligible affinity, with K_i values higher than 10^{-5}M.

Natural PrRP31 and PrRP20, as well as their lipidized analogs palmitoylated PrRP31 (palm-PrRP31) and myristoylated PrRP20 (myr-PrRP20), respectively, increased the phosphorylation of MAPK/ERK1/2 in CHO cells overexpressing GPR10 receptor with an EC_{50} values in the nanomolar range (EC_{50} was 1.01 nM for PrRP31, 5.62 nM for PrRP20, 0.93 nM for palm-PrRP31 and 1.48 nM for myr-PrRP20), which confirmed the powerful agonist effects of palm-PrRP31 and myr-PrRP20 on the GPR10 receptor. The dose–response curves are shown in Supplementary Figure S1.

Lipidized PrRP analogs were bound to CHO cells overexpressing NPFF2 receptor with K_i values of 10^{-8}M range or lower, similar to native PrRP20 and PrRP31 in competition binding with a stable NPFF analog ^{125}I-1DMe (Table 1). Myristoylated and palmitoylated PrRP analogs displaced ^{125}I-1DMe with affinity equal to or higher than 1DMe ($K_i = 2.21 \pm 0.70$).

In the rat tumor pituitary cell line RC-4B/C expressing endogenously both GPR10 and NPFF2, lipidized PrRP analogs were bound with a very high affinity to these cells that increased with the length of the carbon chain of a fatty acid (Table 1).

Palm- and stear-PrRP31 and myr-PrRP20 attenuate food intake after acute peripheral administration in fasted lean mice and activate neurons in the food intake-regulating areas in the brain

Food intake was unaffected in Sal-treated controls and native PrRP31 and native PrRP20 administered SC in mice, both fasted and freely fed (Figure 1). In contrast, anorexigenic effects of several peripherally administered lipidized analogs of PrRP31 and PrRP20 were proven in fasted mice (Figure 1a and b) and freely fed mice (Figure 1c). After the acute SC administration of myr-PrRP20 and palm- and stear-PrRP31 (dose of 5 mg kg^{-1}), food intake was very significantly lowered for several hours. The effects of myr-PrRP20 and palm-PrRP31 were dose-dependent, with a dose as low as 1 mg kg^{-1} of each peptide significantly lowering food intake (Supplementary Figure S2). Scrambled myristoylated PrRP20 had no effect on food intake in mice after peripheral administration (Figure 1a). Interestingly, PrRP31 lipopeptides with myristoyl and fatty acids of shorter carbon chains and PrRP20 lipopeptides with dodecanoyl fatty acid and fatty

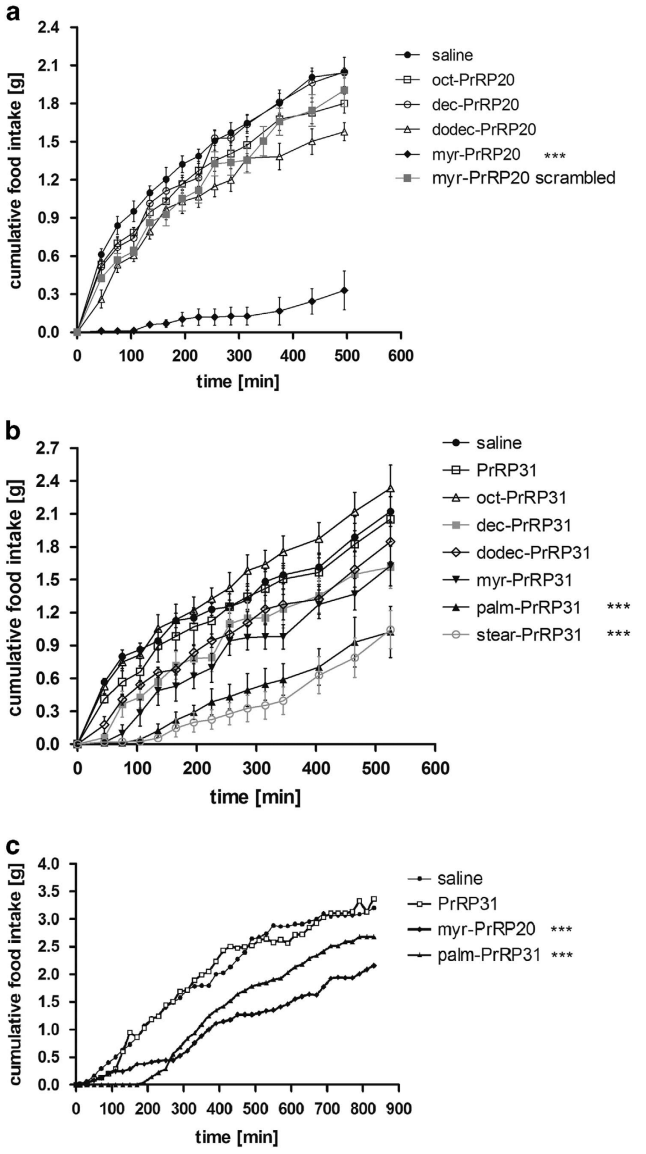

Figure 1. Palmitoylated and stearoylated PrRP31 and myristoylated PrRP20 attenuate food intake after acute peripheral administration in fasted mice. Cumulative food intake of 17 h fasted mice after acute SC administration of (**a**) lipidized PrRP20 analogs, (**b**) natural and lipidized PrRP31 analogs at a dose of 5 mg kg^{-1}, (**c**) cumulative food intake of freely fed mice after acute SC administration of saline, PrRP31, myr-PrRP20 and palm-PrRP31 (dose 5 mg kg^{-1}). Food intake is expressed in grams of food consumed ($n = 6$–8 mice per group). ***$P < 0.001$ vs saline-treated group. The significance concerns the whole time course.

acids of shorter carbon chains did not significantly affect food intake (Figure 1a and b). Although myr-PrRP20 showed a stronger anorexigenic potency at a dose of 5 mg kg^{-1} SC in fasted mice compared with palm-PrRP31 (Figures 1a and b), anorexigenic effect of both analogs was comparable in freely fed mice (Figure 1c) and moreover, palm-PrRP31 lowered food intake more significantly than myr-PrRP30 at a dose of 1 mg kg^{-1} (Supplementary Figure 2). It might be explained by higher lipophilicity and lower solubility of myr-PrRP20 compared with palm-PrRP31.

The central effect of peripherally administered palm-PrRP31 as well as myr-PrRP20 was confirmed by a significant increase in c-Fos immunoreactivity in the hypothalamic and brainstem nuclei involved in food intake regulation (Figure 2). Natural and octanoylated PrRP31 administered peripherally did not influence food intake and did not increase c-Fos immunoreactivity.

Lipidized analogs of PrRP are selective and stable anorexigenic compounds

Several behavioral tests in mice were carried out to evaluate possible side effects of selected PrRP analogs after their peripheral administration. Two analogs that did not affect food intake after SC administration, PrRP31 and oct-PrRP31, and two analogs that did significantly decrease food intake, myr-PrRP20 and palm-PrRP31, were SC administered into mice at a dose of 5 mg kg^{-1} to test their sedative effect (in the open field test), analgesic activity (in the hot plate test) and anxiety (in the elevated plus maze). Neither non-lipidized nor lipidized PrRP analogs influenced open field locomotory activity, nor did they exhibit any analgesic or hyperalgesic activity, nor were any anxiogenic effects in the elevated plus maze observed (Supplementary Figure S3).

After intravenously or SC administration, Palm-PrRP31 did not increase PRL release in rats compared with intravenously administered thyrotropin (Supplementary Figure S4a). Similarly, myr-PrRP20 and palm-PrRP31 did not significantly affect PRL release in mice after SC administration (Supplementary Figure S4b).

The degradation of selected PrRP analogs was tested in rat plasma *in vitro*. The stabilities of palm-PrRP31 and myr-PrRP20 were prolonged (> 24 h) compared with native PrRP20 or PrRP31 (half-lives ~ 10–20 min) (Figure 3a), possibly by promoting the association of these peptides with circulating plasma proteins through the attached fatty-acid moieties.

To further validate the pharmacokinetic profiles of selected analogs *in vivo*, plasma concentrations of PrRP31, PrRP20, palm-PrRP31 and myr-PrRP20 were determined after a single SC injection into mice (Figure 3b). Lipidized PrRP analogs showed longer stability and increased AUC compared with natural PrRP31 and PrRP20.

Chronic 14-days administration of palm-PrRP31 and myr-PrRP20 decreased food intake and body weight in DIO mice, improved metabolic parameters and positively affected lipid metabolism

Rodents with diet-induced obesity are considered models of the most common human obesity, which is associated with the consumption of HF food. The therapeutic potential of two selected lipidized PrRP analogs that were the most potent in the acute food intake test was assessed in diet-induced obese mice that were peripherally administered these peptides for 14-days twice per day. Figure 4 shows that the food intake and body weight in diet-induced obesity (DIO) mice were significantly lowered, mainly by the effect of palm-PrRP31. After the treatment, palm-PrRP31-treated mice weighed ~ 15% less and myr-PrRP20-treated mice ~ 10% less than Sal-treated controls. No signs of inflammation were observed during the treatment.

As shown in Table 2, palm-PrRP31 treatment significantly lowered insulin and leptin levels in blood, and decreased SCAT and perirenal fat masses. The group of mice pair-fed to palm-PrRP31 showed similar metabolic changes, suggesting that the primary effect of palm-PrRP31 is most likely due to food intake regulation. Despite the fact that the treatment of DIO mice with myr-PrRP20 decreased circulating level of leptin significantly, the masses of the dissected fat tissues were not significantly lowered (Table 2).

Plasma corticosterone level significantly increased after myr-PrRP20 and palm-PrRP31 treatment compared with Sal-treated group, but increase in adrenocorticotropic hormone level did not reach significance (Supplementary Figure S5).

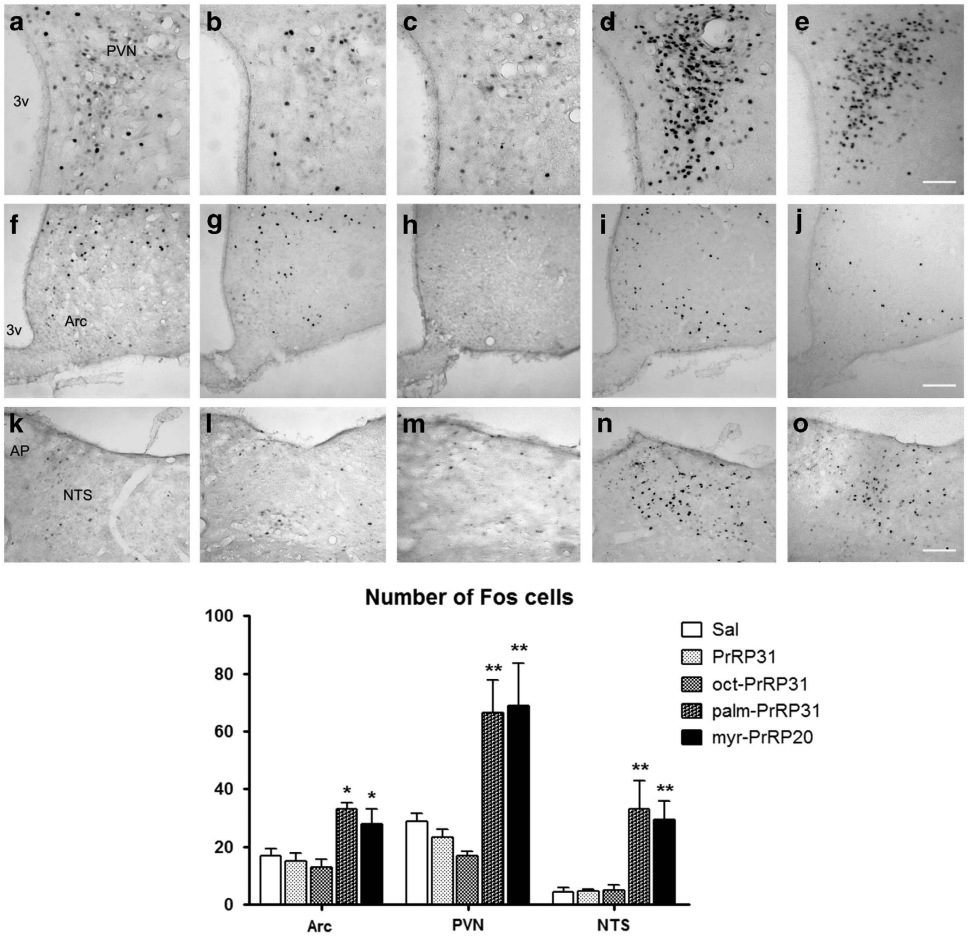

Figure 2. Effect of PrRP lipidization on cells activity in food intake-regulating areas in mouse brain. Fos immunoreactivity: the qualitative as well as quantitative assessment of Fos-immunostained cells in coronal section of PVN (**a**–**e**), Arc (**f**–**j**) and NTS (**k**–**o**) 90 min after SC application of saline (**a**, **f**, **k**) and PrRP31 (**b**, **g**, **l**), oct-PrRP31 (**c**, **h**, **m**), palm-PrRP31 (**d**, **i**, **n**) and myr-PrRP20 (**e**, **j**, **o**) at a dose of 5 mg kg^{-1} in fasted mice ($n = 4$). *$P < 0.05$, **$P < 0.01$ vs saline (Sal), PrRP31 and oct-PrRP31. PVN—paraventricular hypothalamic nucleus, Arc—arcuate hypothalamic nucleus, NTS—solitary tract nucleus, 3v—third brain ventricle. Scale bar is 50 μm for **a**–**e**, 100 μm for **f**–**o**.

Expression of UCP-1 was not changed in brown adipose tissue of palm-PrRP31 compared with Sal-treated group (Supplementary Figure S6).

As palm-PrRP31 treatment had the most attenuating effect on fat stores, we investigated the mRNA expressions of adipokines and fat metabolism-regulating enzymes only in palm-PrRP31-treated DIO mice and their pair-fed group. Decrease in the masses of all particular fats dissected resulted in a very significantly attenuated mRNA expressions of leptin (Supplementary Figure S7) but not adiponectin (not shown). In both SCAT and IPAT, the second most significant site of lipogenesis, fatty-acid synthase mRNA was significantly attenuated. Treatment with palm-PrRP31 did not decrease lipoprotein lipase mRNA expression in SCAT or in IPAT in contrast to the results observed in pair-fed animals (Supplementary Figure S7). Palm-PrRP31 treatment attenuated fat metabolism more significantly in the liver, where the mRNAs of enzymes catalyzing the *de novo* synthesis of fatty acids, ACACA and FASN, were reduced significantly and in addition to a reduction in sterol regulatory element-binding protein mRNA (Supplementary Figure S7).

DISCUSSION

In spite of their low toxicity and few side effects, the clinical potential of natural centrally acting anorexigenic neuropeptides is limited due to their low stability and poor bioavailability under physiological conditions. Our work has shown for the first time that a unique modification of PrRP by lipidization led not only to an increased stability in blood but also enabled to exert PrRP central effect after peripheral administration.

In our previous study,[20] we confirmed the importance of the C terminus, identical for both PrRP20 and PrRP31, for their biological activity. Therefore, the N terminus of both natural peptides, PrRP31 and PrRP20, was lipidized with fatty acids of different lengths to preserve their full biological activity. PrRP31 and PrRP20 lipidized by 8–18 carbon chain fatty acids retained their binding affinities to GPR10 and NPFF2 receptors over-expressed in CHO cells and to tumor cells RC-4B/C endogenously expressing both GPR10 and NPFF2 receptors with affinities similar to natural PrRP31.[20,34] Agonistic properties of the lipidized analogs of PrRP31 and PrRP20 were confirmed by an increased MAPK/EKR1/2 phosphorylation in CHO cells overexpressing GPR10 receptor.

Despite similar binding affinities and agonist character of PrRP lipidized by 8–18 carbons chain fatty acids, only palm- and stear-PrRP31 and myr-PrRP20 highly significantly and dose-dependently lowered food intake in lean overnight-fasted and freely fed mice after SC administration, whereas analogs containing fatty acids with shorter carbon chains and the natural PrRP31 or PrRP20 had no effect on food intake. These findings suggest that only palm- or stear-PrRP31 and myr-PrRP20 were probably able to cross the BBB and exert their central effect on food intake. This conclusion was

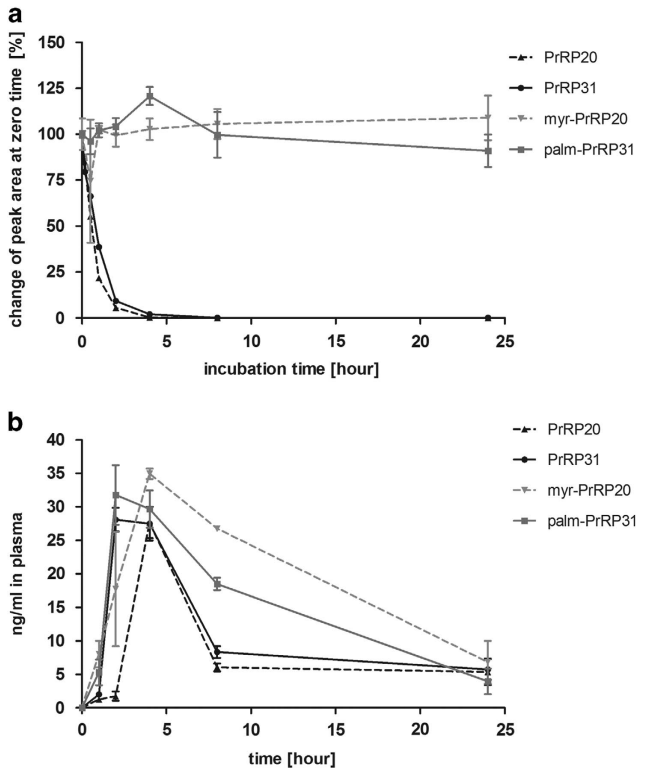

Figure 3. Pharmacokinetics of the PrRP analogs *in vitro* and *in vivo*. (**a**) Degradation profiles in rat plasma. The analog triplicates were incubated for different times in rat plasma and then submitted for immunoanalysis using EIA kit. The results are expressed as the percentage differences from the blood levels of PrRP31 at time 0 with a 10^{-6}M initial concentration. (**b**) Plasma concentrations after single SC injection (5 mg kg^{-1}) in mice ($n=3$) as measured by EIA kit.

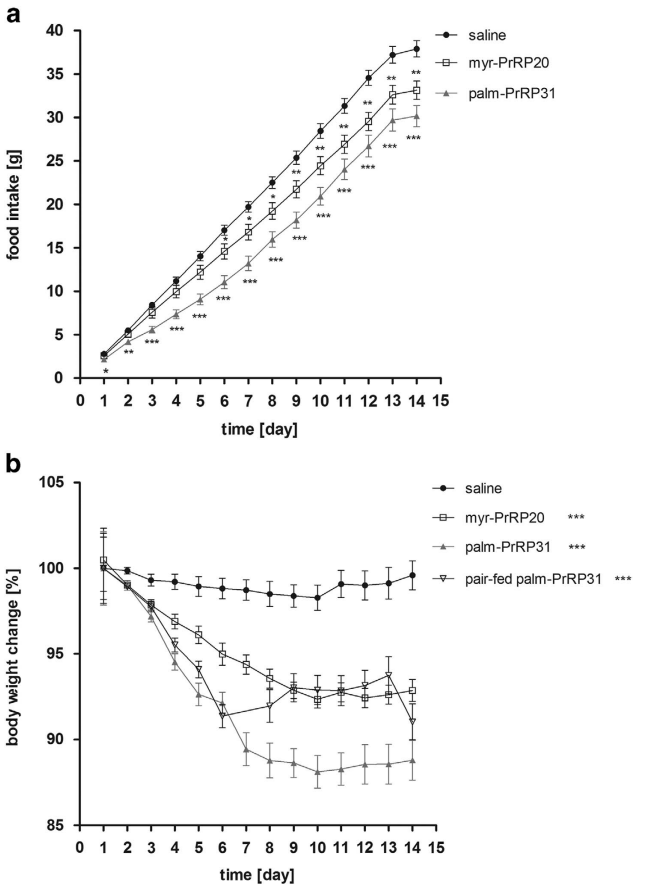

Figure 4. Palmitoylated PrRP31 and myristoylated PrRP20 reduce food intake and body weight of diet-induced obese mice**.** Effect of 14- day administration of palm-PrRP31 and myr-PrRP20 on (**a**) food intake and (**b**) body weight of DIO mice. Mice were SC administered by saline or peptides at a dose of 5 mg kg^{-1} twice daily ($n=10$). Pair-fed group received amount of food consumed by palm-PrRP31-treated group the previous day. The data were analyzed by one-way ANOVA. *$P<0.05$, **$P<0.01$, ***$P<0.001$ vs saline-treated group.

further supported by the fact that both SC administered myr-PrRP20 and palm-PrRP31 significantly enhanced c-Fos immunoreactivity in food intake-regulating hypothalamic and brainstem nuclei containing both GPR10 and NPFF2 receptors,[18,35] whereas natural and octanoylated PrRP31 did not induce these changes.

In the hypothalamus, leptin receptor and PrRP are colocalizated and have additive anorexigenic effect.[36] Anorexigenic effect of PrRP independent of leptin but dependent on CCK was suggested in the brainstem.[37]

The acute SC administration of natural PrRP31, palm-PrRP31 and myr-PrRP20 did not result in any sedative, analgetic or anxiety-inducing effects in mice. Thus, despite their high-affinity binding to NPFF2 receptor, lipidized PrRP analogs do not share the hyperalgesic activities of NPFF.[24] In spite of its name, PrRP-induced PRL release is currently considered controversial.[38] In our experiments, after intravenously or SC administration, palm-PrRP31 or myr-PrRP20 did not increase the release of PRL in rats and mice.

The long-lasting anorexigenic effect of palm- and stear-PrRP31 and myr-PrRP20 analogs could be explained by their prolonged stability owing to binding to serum albumin similar to liraglutide or palmitoylated gastric inhibitory polypeptide.[16] Our stability test confirmed that both palm-PrRP31 and myr-PrRP20 were stable for >24 h in rat plasma. *In vivo* pharmacokinetics in mice also showed longer stability and a higher area under the curve for palm-PrRP31 and myr-PrRP20 compared with natural, non-lipidized analogs.

Finally, the 2-week-long twice daily administration of palm-PrRP31 and myr-PrRP20 to mice with HF diet-induced obesity significantly decreased cumulative food intake and body weight. The time course and the extent of the effect were similar to those of liraglutide,[39,40] confirming the potential of these compounds for obesity treatment.

The decrease in body weight after 2-week palm-PrRP31 treatment in DIO mice was mediated mainly by the reduction of body fat that was accompanied by a decrease in leptin level. Decreased mRNA expressions of fatty-acid synthase in both the adipose tissue and the liver along with a decreased expression of acetyl-CoA carboxylase and sterol regulatory element-binding protein in the liver suggests that this reduction most likely resulted from a decreased *de novo* lipogenesis owing primarily to negative energy balance due to reduced food intake. In our study, changes of UCP-1 mRNA in brown adipose tissue after palm-PrRP31 treatment pointing to possible increase of energy expenditure were not found. On the other hand, significantly increased corticosterone and nonsignificantly increased adreno-corticotropic hormone plasma levels after 14-days treatment with myr-PrRP20 and palm-PrRP31 support the fact that PrRP was proposed to be implicated also in endocrine regulation of hypothalamic–pituitary–andrenal axis.[41]

In conclusion, we have demonstrated that the lipidization of PrRP enabled its central anorexigenic effect after peripheral administration in both acute and chronic settings by enhancing its stability in the blood and improving its ability to cross the BBB. Our data also confirmed that GPR10 and/or NPFF2 receptors are suitable targets for the treatment of obesity. Collectively, our data

Table 2. Metabolic parameters after 14-day SC administration of PrRP analogs in fasted DIO mice

		Group/treatment			
		Saline	*Myr-PrRP20*	*Palm-PrRP31*	*Pair-fed to palm-PrRP31*
Fat/body weight	(%)	16.15 ± 0.4	15.3 ± 0.42	12.7 ± 0.71***	14.5 ± 0.67
SCAT/body weight	(%)	8.07 ± 0.33	7.05 ± 0.19	5.38 ± 0.49***	6.95 ± 0.50
IPAT/body weight	(%)	4.66 ± 0.33	5.09 ± 0.43	4.75 ± 0.19	4.67 ± 0.46
Perirenal fat/body weight	(%)	2.94 ± 0.14	2.77 ± 0.13	2.07 ± 0.20***	2.60 ± 0.08
Liver/body weight	(%)	4.07 ± 0.20	3.60 ± 0.18	3.56 ± 0.07	3.14 ± 0.13***
Leptin	(ng ml^{-1})	53.3 ± 3.49	39.6 ± 3.47*	24.7 ± 3.39***	27.4 ± 1.91***
Glucose	(mmol l^{-1})	6.94 ± 0.28	7.52 ± 0.16	7.26 ± 0.29	5.6 ± 0.37**
Insulin	(ng ml^{-1})	4.09 ± 0.55	3.54 ± 0.47	2.37 ± 0.47*	0.79 ± 0.14***
Triglycerides	(mg dl^{-1})	72.2 ± 3.2	68.7 ± 4.16	66.8 ± 8.74	57.5 ± 5.38

Abbreviations: IPAT, intraperitoneal adipose tissue; SCAT, subcutaneous adipose tissue. All values are expressed as mean ± s.e.m. ($n = 10$ per group). Significance (one-way ANOVA) is *$P < 0.05$, **$P < 0.01$ and ***$P < 0.001$ vs saline-treated group.

suggest that lipidized PrRP analogs have potential as a possible future anti-obesity drugs.

CONFLICT OF INTEREST

The authors declare no conflict of interest.

ACKNOWLEDGEMENTS

This study was supported by the GACR No. P303/10/1368 and P303/12/0576, TACR TE01020028, grant of MSMT (No. 20/2014) and by the ASCR RVO: 61388963 and RVO:67985823. We gratefully acknowledge T Elbert for the radioiodination of peptides and H Vysušilová, Z Kopecká and I Nahodilová for excellent technical assistance.

REFERENCES

1 Hinuma S, Habata Y, Fujii R, Kawamata Y, Hosoya M, Fukusumi S *et al.* A prolactin-releasing peptide in the brain. *Nature* 1998; **393**: 272–276.
2 Ibata Y, Iijima N, Kataoka Y, Kakihara K, Tanaka M, Hosoya *et al.* Morphological survey of prolactin-releasing peptide and its receptor with special reference to their functional roles in the brain. *Neurosci Res* 2000; **38**: 223–230.
3 Lawrence C, Celsi F, Brennand J, Luckman S. Alternative role for prolactin-releasing peptide in the regulation of food intake. *Nat Neurosci* 2000; **3**: 645–646.
4 Engström M, Brandt A, Wurster S, Savola JM, Panula P. Prolactin releasing peptide has high affinity and efficacy at neuropeptide FF2 receptors. *J Pharmacol Exp Ther* 2003; **305**: 825–832.
5 Dockray GJ. The expanding family of -RFamide peptides and their effects on feeding behaviour. *Exp Physiol* 2004; **89**: 229–235.
6 Chartrel N, Bruzzone F, Leprince J, Tollemer H, Anouar Y, Do-Régo JC *et al.* Structure and functions of the novel hypothalamic RFamide neuropeptides R-RFa and 26RFa in vertebrates. *Peptides* 2006; **27**: 1110–1120.
7 Lawrence C, Ellacott K, Luckman S. PRL-releasing peptide reduces food intake and may mediate satiety signaling. *Endocrinology* 2002; **143**: 360–367.
8 Bjursell M, Lennerås M, Göransson M, Elmgren A, Bohlooly-Y M. GPR10 deficiency in mice results in altered energy expenditure and obesity. *Biochem Biophys Res Commun* 2007; **363**: 633–638.
9 Takayanagi Y, Matsumoto H, Nakata M, Mera T, Fukusumi S, Hinuma S *et al.* Endogenous prolactin-releasing peptide regulates food intake in rodents. *J Clin Invest* 2008; **118**: 4014–4024.
10 Maniscalco JW, Rinaman L. Overnight food deprivation markedly attenuates hindbrain noradrenergic, glucagon-like peptide-1, and hypothalamic neural responses to exogenous cholecystokinin in male rats. *Physiol Behav* 2013; **121**: 35–42.
11 Dodd GT, Luckman SM. Physiological Roles of GPR10 and PrRP Signaling. *Front Endocrinol (Lausanne)* 2013; **4**: 20.
12 Bellmann-Sickert K, Beck-Sickinger AG. Peptide drugs to target G protein-coupled receptors. *Trends Pharmacol Sci* 2010; **31**: 434–441.
13 Brasnjevic I, Steinbusch HW, Schmitz C, Martinez-Martinez P. Initiative ENR. Delivery of peptide and protein drugs over the blood-brain barrier. *Prog Neurobiol* 2009; **87**: 212–251.
14 Malavolta L, Cabral FR. Peptides: important tools for the treatment of central nervous system disorders. *Neuropeptides* 2011; **45**: 309–316.
15 Havelund S, Plum A, Ribel U, Jonassen I, Vølund A, Markussen J *et al.* The mechanism of protraction of insulin detemir, a long-acting, acylated analog of human insulin. *Pharm Res* 2004; **21**: 1498–1504.
16 Gault VA, Kerr BD, Harriott P, Flatt PR. Administration of an acylated GLP-1 and GIP preparation provides added beneficial glucose-lowering and insulinotropic actions over single incretins in mice with Type 2 diabetes and obesity. *Clin Sci (Lond)* 2011; **121**: 107–117.
17 Manning S, Pucci A, Finer N. Pharmacotherapy for obesity: novel agents and paradigms. *Ther Adv Chronic Dis* 2014; **5**: 135–148.
18 Roland B, Sutton S, Wilson S, Luo L, Pyati J, Huvar R *et al.* Anatomical distribution of prolactin-releasing peptide and its receptor suggests additional functions in the central nervous system and periphery. *Endocrinology* 1999; **140**: 5736–5745.
19 Boyle R, Downham R, Ganguly T, Humphries J, Smith J, Travers S. Structure-activity studies on prolactin-releasing peptide (PrRP). Analogues of PrRP-(19-31)-peptide. *J Pept Sci* 2005; **11**: 161–165.
20 Maletínská L, Spolcová A, Maixnerová J, Blechová M, Zelezná B. Biological properties of prolactin-releasing peptide analogs with a modified aromatic ring of a C-terminal phenylalanine amide. *Peptides* 2011; **32**: 1887–1892.
21 Blechová M, Nagelová V, Záková L, Demianová Z, Zelezná B, Maletínská L. New analogs of the CART peptide with anorexigenic potency: the importance of individual disulfide bridges. *Peptides* 2013; **39**: 138–144.
22 Maletínská L, Pýchová M, Holubová M, Blechová M, Demianová Z, Elbert T *et al.* Characterization of new stable ghrelin analogs with prolonged orexigenic potency. *J Pharmacol Exp Ther* 2012; **340**: 781–786.
23 Holubová M, Spolcová A, Demianová Z, Sýkora D, Fehrentz JA, Martinez J *et al.* Ghrelin agonist JMV 1843 increases food intake, body weight and expression of orexigenic neuropeptides in mice. *Physiol Res* 2013; **62**: 435–444.
24 Maletinska L, Ticha A, Nagelova V, Spolcova A, Blechova M, Elbert T *et al.* Neuropeptide FF analog RF9 is not an antagonist of NPFF receptor and decreases food intake in mice after its central and peripheral administration. *Brain Res* 2013; **1498**: 33–40.
25 Motulsky H, Neubig R. Analyzing radioligand binding data. *Curr Protoc Neurosci* 2002; **Chapter 7**: Unit 7.5.
26 Nagelová V, Pirník Z, Železná B, Maletínská L. CART (cocaine- and amphetamine-regulated transcript) peptide specific binding sites in PC12 cells have characteristics of CART peptide receptors. *Brain Res* 2014; **1547**: 16–24.
27 Pirnik Z, Bundziková J, Holubová M, Pýchová M, Fehrentz JA, Martinez J *et al.* Ghrelin agonists impact on Fos protein expression in brain areas related to food intake regulation in male C57BL/6 mice. *Neurochem Int* 2011; **59**: 889–895.
28 Maletínská L, Maixnerová J, Matysková R, Haugvicová R, Pirník Z, Kiss A *et al.* Synergistic effect of CART (cocaine- and amphetamine-regulated transcript) peptide and cholecystokinin on food intake regulation in lean mice. *BMC Neurosci* 2008; **9**: 101.
29 Maletínská L, Lignon M, Galas M, Bernad N, Pírková J, Hlavácek J *et al.* Pharmacological characterization of new cholecystokinin analogues. *Eur J Pharmacol* 1992; **222**: 233–240.
30 Kopecký J, Hodný Z, Rossmeisl M, Syrový I, Kozak LP. Reduction of dietary obesity in aP2-Ucp transgenic mice: physiology and adipose tissue distribution. *Am J Physiol* 1996; **270**: E768–E775.
31 Maletinska L, Matyskova R, Maixnerova J, Sykora D, Pychova M, Spolcova A *et al.* The Peptidic GHS-R antagonist [D-Lys(3)]GHRP-6 markedly improves adiposity and related metabolic abnormalities in a mouse model of postmenopausal obesity. *Mol Cell Endocrinol* 2011; **343**: 55–62.

32 Chang C, Cheng Y. Ribonucleotide reductase isolated from human cells. Heterogeneity among the sources. *Biochem Pharmacol* 1978; **27**: 2297–2300.
33 Maixnerová J, Hlavácek J, Blokesová D, Kowalczyk W, Elbert T, Sanda *et al*. Structure-activity relationship of CART (cocaine- and amphetamine-regulated transcript) peptide fragments. *Peptides* 2007; **28**: 1945–1953.
34 Maixnerová J, Špolcová A, Pýchová M, Blechová M, Elbert T, Rezáčová *et al*. Characterization of prolactin-releasing peptide: binding, signaling and hormone secretion in rodent pituitary cell lines endogenously expressing its receptor. *Peptides* 2011; **32**: 811–817.
35 Gouardères C, Faura CC, Zajac JM. Rodent strain differences in the NPFF1 and NPFF2 receptor distribution and density in the central nervous system. *Brain Res* 2004; **1014**: 61–70.
36 Ellacott KL, Halatchev IG, Cone RD. Characterization of leptin-responsive neurons in the caudal brainstem. *Endocrinology* 2006; **147**: 3190–3195.
37 Bechtold DA, Luckman SM. Prolactin-releasing Peptide mediates cholecystokinin-induced satiety in mice. *Endocrinology* 2006; **147**: 4723–4729.
38 Jarry H, Heuer H, Schomburg L, Bauer K. Prolactin-releasing peptides do not stimulate prolactin release *in vivo*. *Neuroendocrinology* 2000; **71**: 262–267.
39 Porter DW, Kerr BD, Flatt PR, Holscher C, Gault VA. Four weeks administration of Liraglutide improves memory and learning as well as glycaemic control in mice with high fat dietary-induced obesity and insulin resistance. *Diabetes Obes Metab* 2010; **12**: 891–899.
40 Kerr BD, Flatt PR, Gault VA. Effects of gamma-glutamyl linker on DPP-IV resistance, duration of action and biological efficacy of acylated glucagon-like peptide-1. *Biochem Pharmacol* 2010; **80**: 396–401.
41 Maruyama M, Matsumoto H, Fujiwara K, Noguchi J, Kitada C, Fujino *et al*. Prolactin-releasing peptide as a novel stress mediator in the central nervous system. *Endocrinology* 2001; **142**: 2032–2038.

Supplementary Information accompanies this paper on International Journal of Obesity website (http://www.nature.com/ijo)

Journal of Alzheimer's Disease 45 (2015) 823–835
DOI 10.3233/JAD-143150
IOS Press

Anorexigenic Lipopeptides Ameliorate Central Insulin Signaling and Attenuate Tau Phosphorylation in Hippocampi of Mice with Monosodium Glutamate-Induced Obesity

Andrea Špolcová[a,b], Barbora Mikulášková[a], Martina Holubová[a], Veronika Nagelová[a], Zdenko Pirnik[a,e,f], Jana Zemenová[a,d], Martin Haluzík[c], Blanka Železná[a], Marie-Christine Galas[b] and Lenka Maletínská[a,*]

[a]*Institute of Organic Chemistry and Biochemistry, AS CR, Prague, Czech Republic*
[b]*INSERM UMR837, Lille, France, Jean Pierre Aubert Research Centre, Faculté de Médecine-Pòle Recherche, Institut de Médecine Prédictive et de Recherche Thérapeutique, Université Droit et Santé de Lille, CHU-Lille, Lille, France*
[c]*Third Department of Medicine, First Faculty of Medicine, Charles University in Prague, Prague, Czech Republic*
[d]*Institute of Chemical Technology, Department of Analytical Chemistry, Prague, Czech Republic*
[e]*Laboratory of Functional Neuromorphology, Institute of Experimental Endocrinology, SAS, Bratislava, Slovak Republic*
[f]*Department of Human and Clinical Pharmacology, University of Veterinary Medicine, Košice, Slovak Republic*

Accepted 29 December 2014

Abstract. Numerous epidemiological and experimental studies have demonstrated that patients who suffer from metabolic disorders, such as type 2 diabetes mellitus (T2DM) or obesity, have higher risks of cognitive dysfunction and of Alzheimer's disease (AD). Impaired insulin signaling in the brain could contribute to the formation of neurofibrillary tangles, which contain an abnormally hyperphosphorylated tau protein. This study aimed to determine whether potential tau hyperphosphorylation could be detected in an obesity-induced pre-diabetes state and whether anorexigenic agents could affect this state. We demonstrated that 6-month-old mice with monosodium glutamate (MSG) obesity, which represent a model of obesity-induced pre-diabetes, had increased tau phosphorylation at Ser396 and Thr231 in the hippocampus compared with the controls, as determined by western blots. Two weeks of subcutaneous treatment with a lipidized analog of prolactin-releasing peptide (palm-PrRP31) or with the T2DM drug liraglutide, which both had a central anorexigenic effect, resulted in increased phosphorylation of the insulin cascade kinases PDK1 (Ser241), Akt (Thr308), and GSK-3β (Ser9). Furthermore, these drugs attenuated phosphorylation at Ser396, Thr231, and Thr212 of tau and of the primary tau kinases in the hippocampi of 6-month-old MSG-obese mice. We identified tau hyperphosphorylation in the obesity-induced pre-diabetes state in MSG-obese mice and demonstrated the beneficial effects of palm-PrRP31 and liraglutide, both of known central anorexigenic effects, on hippocampal insulin signaling and on tau phosphorylation.

Keywords: Alzheimer's disease, insulin signaling, liraglutide, monosodium glutamate-obese mice, obesity, pre-diabetes, prolactin-releasing peptide, tau phosphorylation

INTRODUCTION

Besides extracellular amyloid-β peptide (Aβ) plaques, Alzheimer's disease (AD) is characterized by intracellular hyperphosphorylated tau protein

*Correspondence to: Dr. Lenka Maletínská, Institute of Organic Chemistry and Biochemistry AS CR, Flemingovo nam. 2, 166 10 Prague 6, Czech Republic. Tel.: +420 220183567; Fax: +420 220183571; E-mail: maletin@uochb.cas.cz.

ISSN 1387-2877/15/$35.00

neurofibrillary tangles. Tau protein is expressed mainly in neurons where it promotes tubulin assembling to microtubules and establishes links between microtubules and other cytoskeleton components. Binding of tau to tubulin is regulated by phosphorylation of tau. Hyperphosphorylation lowers binding of tau to tubulin and promotes tau self-polymerization and aggregation to neurofibrillary tangles [1–3]. Tau is primarily phosphorylated by the following proline-directed kinases: GSK-3β (glycogen synthase kinase-3β), cdk5 (cyclin-dependent kinase 5), p44/42 MAPK/ERK1/2 (mitogen-activated protein kinases/extracellular signal-regulated kinases), and JNK (c-Jun N-terminal kinase) [4]. When tau and its various kinases were co-overexpressed in neuroblastoma cells, GSK-3α, GSK-3β, and MAPK 13 were the most effective tau kinases that phosphorylated Ser202, Thr231, Ser235, and Ser396/404, which represent the AD-relevant phosphorylation sites. Generally, GSK-3β has a kinase activity to the most phosphorylation sites of tau. Most of the kinases phosphorylate several tau epitopes, and most phosphorylation sites are targets of more than one kinase. Additionally, some epitopes can be phosphorylated only after other sites have been phosphorylated [5, 6].

GSK-3β is a participant in the insulin signaling cascade and is abundantly expressed in the central nervous system. The phosphorylation of serines 9 and 389 inhibits the kinase activity of GSK-3β [7]. Decreased insulin effectiveness with attenuated GSK-3β Ser9 phosphorylation was shown to result in enhanced GSK-3β kinase activity toward tau in both type 2 diabetes mellitus (T2DM) and AD patients [8]. Similarly, in db/db mice, which represent a rodent model of T2DM, hippocampal tau protein phosphorylation at the epitopes Ser199/202, Thr231, and Ser396, as well as spatial memory impairment, increased progressively with age-related hyperinsulinemia and hyperglycemia [9, 10]. The pathological changes in GSK-3β and tau phosphorylation identified in db/db mice were reversed with insulin administration [11].

Insulin secretagogues, such as the glucagon-like peptide-1 (GLP-1) analogs exendin-4 and liraglutide, which are used for T2DM treatment, as well as the glucose-dependent insulinotropic polypeptide (GIP) analog, have demonstrated protective effects in the brain by reducing Aβ plaques and by preventing the loss of synapses and memory impairments in AD mouse models [12–16]. In rats with intracerebroventricular (ICV) streptozotocin (STZ) treatment-induced sporadic AD [17], a decline in learning and memory and an increase in total and phosphorylated tau in the hippocampus were reversed by an ICV co-application of a GLP-1 analog [18]. Because the central effects of liraglutide have been shown to be exclusively anorexigenic and weight-attenuating [19], one question that arises is whether an anorexigenic neuropeptide produced and acting in the brain, such as prolactin-releasing peptide (PrRP) (reviewed by [20]), could affect tau phosphorylation in the hippocampus. PrRP production is under the control of leptin; PrRP-expressing neurons contain leptin receptors, and when PrRP and leptin were ICV co-administered to rats, these drugs had additive anorexigenic and energy expenditure-increasing effects [21]. The neuroprotective properties of leptin include lowering tau phosphorylation in tau-overexpressing SH-SY5Y cells [22]. Leptin attenuated Aβ formation and improved cognitive performance in CRND8 mice overexpressing amyloid-β precursor protein (AβPP) [23, 24]. A non-functioning leptin receptor was the cause of worsened spatial memory in Zucker diabetic fatty rats [25] and in db/db mice [26].

In this study, we aimed to determine whether tau hyperphosphorylation could be detected during the pre-diabetes state, which is a frequent condition in elderly individuals. A useful rodent model of pre-diabetes includes mice or rats with obesity induced by monosodium glutamate (MSG) subcutaneous injections administered to newborns, which result in specific lesions in the arcuate nucleus (ARC) of the hypothalamus. MSG-obese rodents develop obesity with increased adiposity at a sustained body weight [27] because of a lower metabolic rate rather than elevated food intake [28]. Hyperinsulinemia at nearly normoglycemia [29] supports the use of MSG- obese mice as a model of pre-diabetes.

In this study, we also aimed to determine how repeated administration of the GLP-1 agonist liraglutide, which is an anti-T2DM drug promoting insulin secretion that has also a central body weight-reducing effect, and our unique centrally acting anorexigenic lipidized PrRP analog, affected metabolic parameters connected with pre-diabetes in the periphery and insulin signaling and tau phosphorylation in the hippocampus.

MATERIALS AND METHODS

Peptides

The palmitoylated PrRP analog palm-PrRP31 (N-palm-SRTHRHSMEIRTPDINPAWYASRGIRPVG RF-NH_2) was synthesized and purified at the Institute

of Organic Chemistry and Biochemistry, Prague, Czech Republic as previously described [30]. PrRP lipidization was performed as previously described in [31] on a fully protected peptide on resin as the final step. The purity and identity of the peptide was determined using analytical HPLC and a Q-TOF micro MS technique (Waters, Milford, MA, USA).

Liraglutide (Victoza, Novo Nordisk, Maloev, Denmark, 6 mg/ml in an injection pen) was obtained from a pharmacy.

Experimental animals

All animal experiments followed the ethical guidelines for animal experiments and the Czech Republic Act No. 246/1992. The experiments were approved by the Committee for Experiments with Laboratory Animals of the Academy of Sciences of the Czech Republic.

NMRI mice (Charles River, Sulzfeld, Germany) were housed at 23°C with a daily 12-h light and dark cycle (lights on at 6 a.m.). The mice had free access to water and a standard chow diet (Mlýn Kocanda, Jesenice, Czech Republic), which contained 25%, 9%, and 66% calories as protein, fat, and carbohydrates, respectively, and 3.4 kcal/g energy content.

For MSG-induced obesity, newborn male NMRI mice were subcutaneously (SC) administered L-glutamic acid sodium salt hydrate (Sigma-Aldrich, St. Louis, MO, USA) (4 mg/g body weight) at postnatal days 2–8 as previously described [28].

Body weight was monitored once per week up to the age of 6 months. Overnight fasted MSG-obese mice and their controls at ages 2 and 6 months ($n = 10$) were sacrificed by decapitation starting at 8:00 a.m. The trunk blood was collected, and the plasma was separated and stored at −20°C. The white adipose tissue (i.e., subcutaneous, abdominal, and perirenal fat), the liver and the hippocampus of all mice were dissected and weighed. The rate of adiposity was expressed as the fat-to-body weight ratio (the ratio of the total adipose tissue weight to the total body weight).

Effects of 14-day administration of palm-PrRP31 and liraglutide on body weight, food intake, metabolic parameters, insulin signaling, and tau phosphorylation in MSG-obese mice

At 6 months old, one week before the beginning of the experiment, the MSG-obese mice were randomly divided into groups of 10 mice and placed in individual cages with free access to food and water. The following week, the mice were subjected to a 14-day administration of peptides. Three groups were SC injected with saline, palm-PrRP31 (5 mg/kg), or liraglutide (0.2 mg/kg, both peptides dissolved in saline) twice per day (at 8:00 a.m. and 6:00 p.m.). The amount of food consumed and the weights of the mice were monitored daily.

At the end of the experiment, overnight fasted mice were sacrificed by decapitation starting at 8:00 a.m. Blood was collected, and tissues were dissected as previously described in section Experimental animals.

Glucose tolerance test

An intraperitoneal glucose tolerance test (IPGTT) was performed on day 9 of the 14-day treatment. Overnight fasted MSG-obese mice were IP injected with glucose (2 g/kg) at 8:00 a.m. (time 0). Then, blood glucose was measured at 0, 15, 30, 60, 90, 120, and 180 min following injection using a Glucocard glucometer (Arkray, Kyoto, Japan).

Determination of hormonal and biochemical parameters

The plasma insulin concentrations were measured using RIA (Millipore, St. Charles, MI, USA and Linco Research, St. Charles, MI, USA), and the leptin concentrations were determined using ELISA (Millipore, St. Charles, MI, USA). The serum glucose levels were measured using a Glucocard glucometer. All measurements were performed according to the protocols recommended by the manufacturers.

Antibodies used for immunoblotting and immunohistochemistry

The following antibodies were used: phospho-PDK1 (3-phosphoinositide-dependent kinase 1) rabbit mAb, PDK1 rabbit mAb, phospho-Akt (Thr308) rabbit mAb, phospho-Akt (Ser473) rabbit mAb, Akt rabbit mAb, phospho-GSK-3β (Ser9) rabbit mAb, GSK-3 β rabbit mAb, phospho-MAPK/ERK1/2 mouse mAb, total MAPK/ERK1/2 mouse mAb, phospho-JNK rabbit mAb, total JNK rabbit mAb, anti-mouse IgG HRP-linked antibody, anti-rabbit IgG horseradish peroxidase (HRP)-linked antibody (purchased from Cell Signaling Technology, Beverly, MA, USA). Anti-Tau[pSer^{396}] rabbit mAb, anti-Tau[pThr^{231}] rabbit mAb were purchased from Invitrogen, NY, USA and AT8 antibody was purchased from Thermo Scientific, Waltham, MA, USA. Tau CTer mouse mAb was

identified previously [32] and anti-β-actin antibody produced in mouse were obtained from Sigma-Aldrich, St. Louis, MO, USA.

Tissue preparation for immunoblotting

The hippocampi were separated from the dissected brains and homogenized in cold lysis buffer (62.5 mM Tris-HCl buffer with pH 6.8, 1% deoxycholate, 1% Triton X-100, 50 mM NaF, 1 mM Na_3VO_4 and complete protease inhibitor (Roche Applied Science, Mannheim, Germany)) using a Bullet Blender homogenizer (Next Advance, Inc., Averill Park, NY, USA). During tissue handling, all samples were kept on ice. The lysates were sonicated for 1 min. The protein concentration was determined using a Pierce BCA protein assay kit (Thermo Fisher Scientific, Inc., Waltham, MA, USA). The lysates were diluted to a final concentration of 1 μg/μl in Laemmli sample buffer (62.5 mM Tris-HCl with pH 6.8, 2% SDS, 10% glycerol, 0.01% bromophenol blue, 5% β-mercaptoethanol, 50 mM NaF, and 1 mM Na_3VO_4) and stored at −20°C.

Immunoblotting

The samples for immunoblotting were sonicated for 1 min and boiled at 100°C for 2 min. Then, 10 μg/10μl of each sample was resolved using 5/10% SDS-PAGE electrophoresis. The proteins were transferred onto a nitrocellulose membrane, blocked in 5% non-fat milk or BSA in TBS/Tween-20 buffer (20 mM Tris, 136 mM NaCl, 0.1% Tween-20, 50 mM NaF, and 5 mM Na_3VO_4) and incubated overnight in the corresponding antibody diluted in 5% non-fat milk or 5% BSA in TBS/Tween-20 buffer at 4°C. After incubation for 1 h with a HRP-linked secondary antibody at room temperature, the membranes were developed using Luminata Classico/Crescendo/Forte Western HRP Substrates (Merck Millipore, Darmstadt, Germany), visualized in a ChemiDoc™ System (Bio-Rad, Hercules, CA, USA) and quantified using Image Lab Software (Bio-Rad, Hercules, CA, USA). To compare obtained data the electrophoresis and transfer were performed at the same time in one electrophoretic or transfer system and membranes were visualized in the ChemiDoc™ System altogether. The protein level was normalized to β-actin as a housekeeping protein.

Tissue preparation for immunohistochemistry

One hemisphere of each brain was fixed for 24 h in 4% paraformaldehyde, transferred to 70% ethanol and embedded in paraffin at the histology laboratory of the Faculty of Medicine, Lille, France (Laboratoire d'histologie, Faculté de Médecine, Lille, France).

Phosphorylated tau immunohistochemistry

Five-micrometer thick paraffin-embedded sagittal brain slices were deparaffinized by washing three times in toluene, rehydrated in ethanol (100, 95, 70, and 30%) and unmasked by boiling for 10 min in citrate buffer pH 6 (3.75 mM acid citrate, 2.5 mM disodium phosphate). After 1 h of blocking in 1% horse serum in PBS buffer (Sigma-Aldrich, St. Louis, MO, USA), the slices were incubated overnight at 4°C with the appropriate antibody diluted in PBS/0.2% Triton X-100 buffer. Then, the slices were incubated for 1 h with secondary antibody Alexa 488 or Alexa 568 (Life Technologies, NY, USA). The nuclei were stained with Vectashield/DAPI (4′,6-diamidino-2-phenylindole, Vector Laboratories, Burlingame, CA, USA). Images were acquired on a Zeiss confocal laser-scanning microscope LSM 710 using a 488-nm Argon laser, a 561-nm diode-pumped solid-state laser and a 405-nm ultraviolet laser with the same laser intensities to compare the images at Lille 2 University (Plate-forme d'Imagerie Moléculaire et Cellulaire).

Prolactin releasing hormone receptor (PrRP-R) immunohistochemistry

Overnight fasted untreated control male NMRI mice ($n = 4$, body weight 45.6 ± 1.3 g) with the free access to water were used for PrRP-R immunohistochemical processing. The mice were deeply anesthetized with sodium pentobarbital (50 mg/kg, IP) and transcardially perfused with 0.1 M phosphate buffer (PB, pH 7.4) containing 4% paraformaldehyde. The brains were subsequently removed, postfixed in the same fixative overnight at 4°C, and infiltrated with 20% sucrose in 0.1 M PB for 48 h at 4°C. The brains were cut into 30-μm thick coronal sections at −22°C in a Leica CM1950 cryostat (Leica Microsystems GmbH, Germany), and the free-floating sections were collected in cold (4°C) PB.

The free-floating sections were repeatedly washed in cold PB, followed by preincubation in 3% H_2O_2 for 40 min at room temperature. Then, the sections were incubated with rabbit PrRP-R polyclonal antiserum (1:200, LifeSpan BioSciences, Inc., LS-C177303) and diluted in 0.1 M PB containing 4% normal goat serum (Gibco, Grand Island, NY, USA), 0.5% Triton X-100 (Sigma-Aldrich, St. Louis, MO, USA), and 0.1%

sodium azide for 48 h at 4°C. After several rinses in PB, the sections were incubated with biotinylated goat anti-rabbit IgG (1:500, VectorStain Elite ABC, Vector Laboratories, Burlingame, CA, USA) diluted in 0.1 M PB containing 4% NGS and 1% Triton X-100 for 90 min at room temperature. The PB rinses were followed by incubation with the avidin-biotin peroxidase complex (1:250, VectorStain Elite ABC, Vector Laboratories, Burlingame, CA), which was diluted in 0.1 M PB containing 1% Triton X-100 for 90 min at room temperature. PB washing was followed by a wash in 0.05 M Tris-HCl (pH 6.0). The PRLHR antigenic sites were visualized with 0.01% 3,3′-diaminobenzidine tetrahydrochloride (DAB, Sigma-Aldrich, St. Louis, MO, USA) dissolved in 0.05 M Tris-HCl containing 0.0012% H_2O_2 for 3–5 min. Finally, the sections were mounted on glass, air-dried, and coverslipped with DPX mounting medium (Thermo Fisher Scientific, Inc., Waltham, MA, USA). Immunostaining of the negative control, which did not display antiserum immunolabeling, included the substitution of the primary antiserum with normal rabbit serum and the sequential elimination of the primary or secondary antibody from the staining series. The PrRP-R immunoreactive cells were evaluated separately in each side of the coronal sections ($n = 2$-3 sections per mouse) within the dentate gyrus and the CA1-CA3 fields of the hippocampus of the hippocampal formation (from bregma −1.46 to −1.94 mm) according to the mouse brain atlas [33]. Images of representative sections were acquired using a digital camera (Olympus DP70) and an Olympus AX70 light microscope.

Statistical analyses

The data are presented as the means ± SEM for the number of animals indicated in the Figures and Tables. The data were analyzed using a two-way analysis of variance (ANOVA), followed by a Bonferroni *post-hoc* test, or using a one-way ANOVA, followed by a Dunnett's *post-hoc* test or a *t*-test, as stated in the Figure and Table legends, using Graph-Pad Software (San Diego, CA, USA). $p < 0.05$ was considered statistically significant.

RESULTS

Six-month-old MSG-obese mice developed increased tau phosphorylation

The male MSG-obese mice and their age-matched controls were characterized by fat and body weight and by the metabolic parameters connected with obesity and diabetes at 2 and 6 months old (Table 1). The body weights of the MSG-obese mice did not significantly differ from their age-matched controls at 2 or 6 months old. However, the total amount of white adipose tissue and the resultant leptin levels were significantly higher in the MSG-obese mice compared with those amounts and levels of their age-matched controls. Fasting glucose levels were not significantly increased in the MSG-obese mice, whereas the insulin levels were significantly higher in the MSG-obese mice at both 2 and 6 months old compared with those levels of their age-matched controls (Table 1). Thus, the MSG-obese mice exhibited obesity with significant fat accumulation in a pre-diabetes state (increase in insulin but not glucose levels).

The phosphorylation of inhibitory Ser9 in GSK-3β, which is the primary tau kinase, significantly decreased only in the 6-month-old controls compared with that in the 2-month-old controls (Fig. 1). Compared with the controls, the 6-month-old MSG-obese mice displayed increased phosphorylation at the Ser396 and Thr231 epitopes of hippocampal tau, whereas the 2-month-old MSG-obese mice did not display different phosphorylation levels of the Ser396 and Thr231 epitopes of hippocampal tau compared with respective age-matched controls (Fig. 1). It was the reason why 6-month-old MSG-obese mice were used in the following experiment.

Table 1
Metabolic parameters of 2 and 6 months old MSG mice and their age-matched controls

Mice	Body weight [g]	White adipose tissue [% body weight]	Glucose [mmol/l]	Insulin [ng/ml]	Leptin [ng/ml]
Controls 2 months	40.29 ± 0.94	4.54 ± 0.47	6.63 ± 0.46	0.96 ± 0,15	2.07 ± 0.43
MSG 2 months	42.50 ± 0.59	12.04 ± 0.63***	8.55 ± 0.34	3.48 ± 0.57*	27.38 ± 4.14**
Controls 6 months	53.73 ± 1.84	6.88 ± 0.47	6.43 ± 0.52	0.83 ± 0.27	4.03 ± 1.55
MSG 6 months	57.18 ± 1.26	11.46 ± 0.48 ###	5.83 ± 0.45	3.64 ± 0.99#	18.11 ± 2.91##

Data are mean ± SEM ($n = 10$ animals per group). Significance is *$p < 0.05$, **$p < 0.01$, and ***$p < 0.001$ (*versus control 2 months, #versus control 6 months) using one-way ANOVA, Bonferroni *post hoc* test.

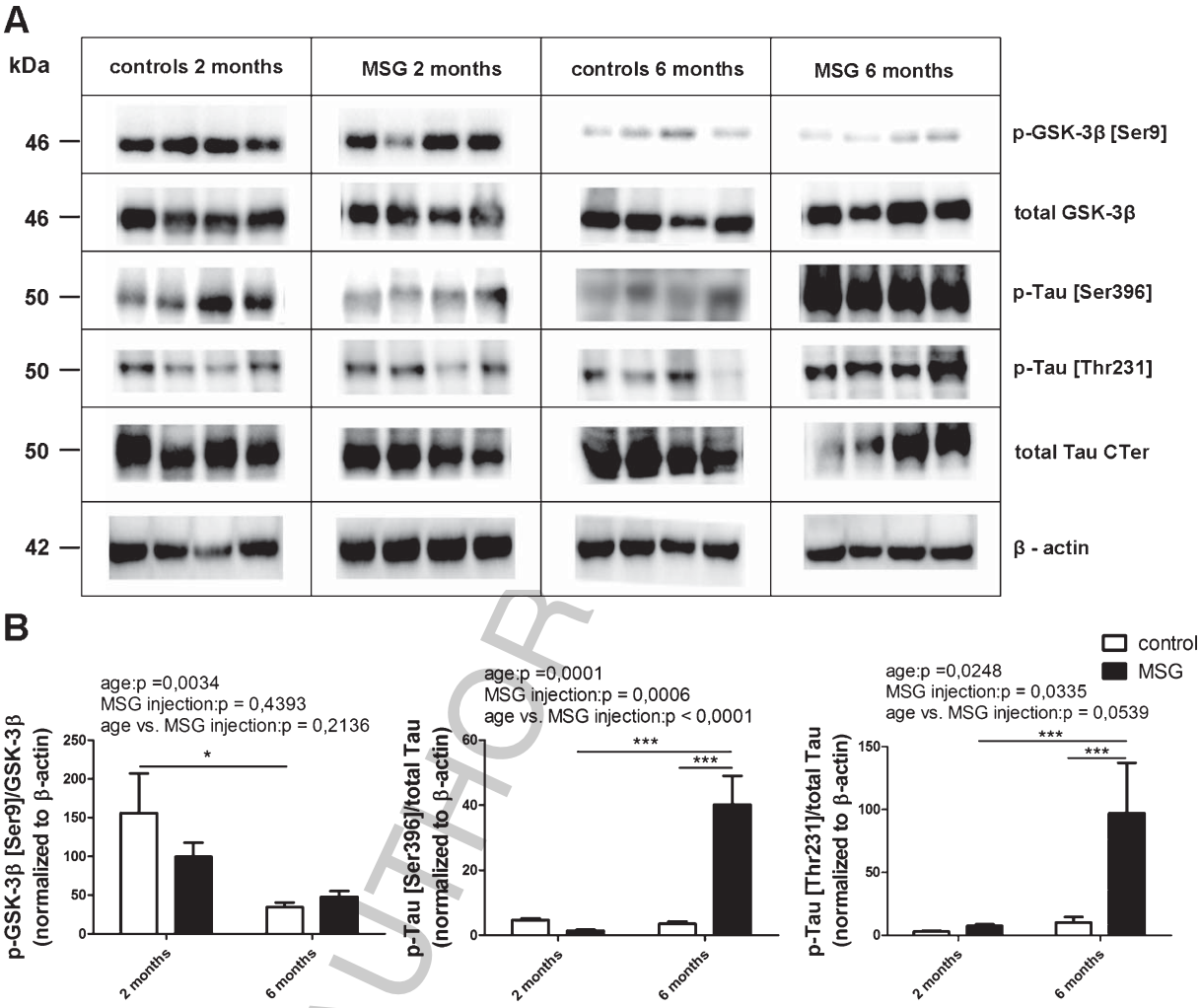

Fig. 1. MSG mice show age-related pathological tau hyperphosphorylation in the hippocampus. A) Western blot analysis of glycogen synthase kinase-3β (GSK-3β) activation and tau phosphorylation (Ser396 and Thr231 epitopes) in hippocampi lysates of 2- and 6-month-old MSG mice and their controls ($n = 10$ mice per group). B) Densitometric quantification of the Western blots normalized to β-actin. Data were analyzed by two-way ANOVA, Bonferroni *post hoc* test. Data are mean ± SEM, $n = 10$ mice per group.

Anorexigenic lipopeptides, palm-PrRP31 and liraglutide, attenuated food intake but did not affect body weight or related metabolic parameters in MSG-obese mice

To examine the effects of two anorexigenic peptides on hippocampal tau phosphorylation in 6-month-old MSG-obese mice, liraglutide and the novel analog palm-PrRP31 were SC administered twice per day for 14 days at doses that significantly lowered food intake and activated neurons in the brain areas regulating food intake after acute administration [34].

The cumulative food intake significantly decreased after treatment with both lipopeptides (Fig. 2). Weight loss did not reach significance after treatment with either palm-PrRP31 or liraglutide compared with that of the saline-treated group (Fig. 2). However, significant weight loss occurred in the saline-treated group most likely because of the repeated injections. Furthermore, based on our previous experience, the NMRI mouse strain is extremely sensitive to manipulation and to repeated injections. The white adipose tissue weight and leptin levels only tended to decrease after treatment with both peptides. The fasting glucose and insulin levels did not significantly differ from those levels of the saline-treated controls (Table 2).

IPGTT was performed in fasted mice on day 9 of the experiment (Fig. 3). The AUCs of palm-PrRP31 or liraglutide treated MSG-obese mice did not significantly differ from those AUCs for the saline-treated

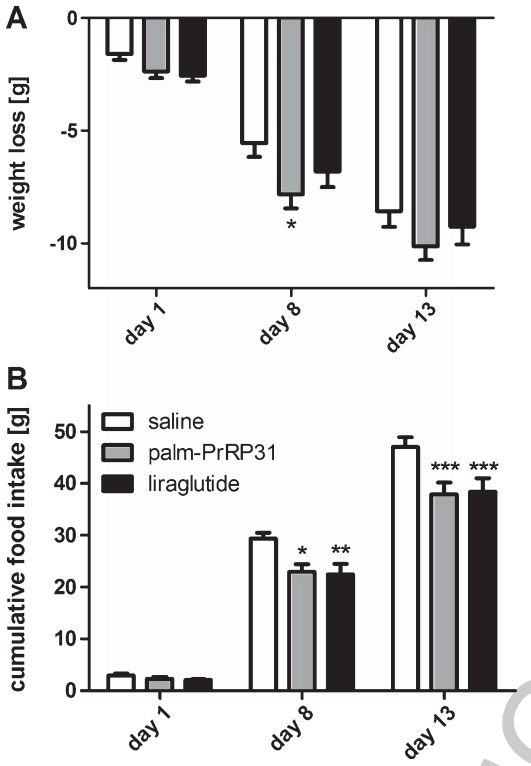

Fig. 2. Body weight change and food intake in MSG mice after palm-PrRP31 or liraglutide treatment. Effect of 14-day administration of liraglutide and palm-PrRP31 on (A) body weight change and (B) food intake of MSG mice. Mice were SC administered by saline or peptides, palm-PrRP31 at a dose of 5 mg/kg and liraglutide at a dose of 0.2 mg/kg twice daily ($n = 10$). The data were analyzed by one-way ANOVA, Bonferroni *post-hoc* test. $^{*}p < 0.05$, $^{**}p < 0.001$ and $^{***}P < 0.001$ vs saline-treated group.

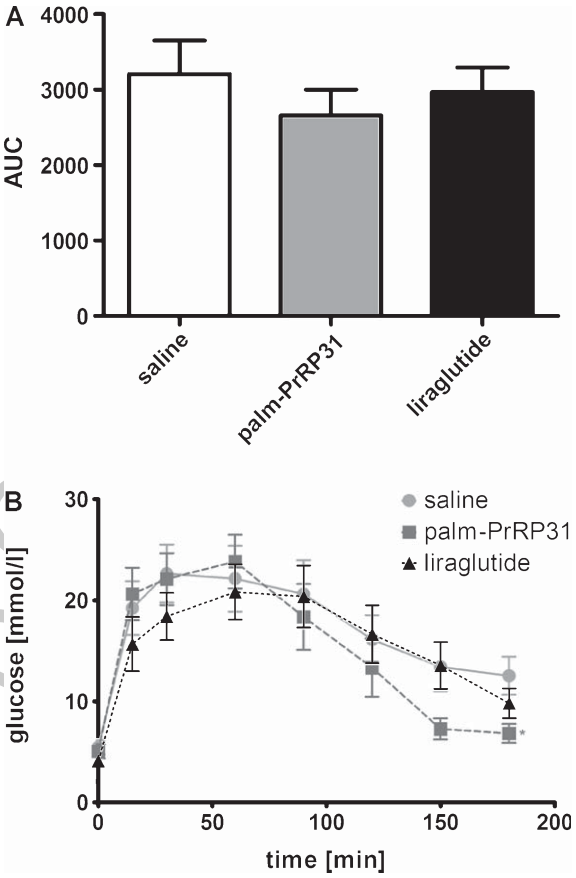

Fig. 3. Glucose tolerance test in MSG mice and their controls. Intraperitoneal glucose tolerance test (IPGTT) was performed in overnight fasted MSG mice injected IP with glucose (2 g/kg) after 9 days of saline, liraglutide, or palm-PrRP31 treatment ($n = 10$). A) Area under curve (AUC). B) Time course of IPGTT. Significance is $^{*}p < 0.05$ using one-way ANOVA, Bonferroni *post-hoc* test.

MSG-obese mice or for the control mice (Fig. 3a); only the final glucose level was significantly lower in the MSG-obese mice treated with palm-PrRP31 compared with the MSG-obese control mice treated with saline (Fig. 3b).

Palm-PrRP31 and liraglutide ameliorated insulin signaling and attenuated activity of tau kinases in the hippocampi of MSG-obese mice

The repeated administration of both palm-PrRP31 and liraglutide positively affected the hippocampal insulin signaling cascade. Figure 4 shows significant enhancement of PDK phosphorylation in the liraglutide-treated mice but not after palm-PrRP31 intervention. Akt phosphorylation at the Thr308 epitope significantly increased in the palm-PrRP31-treated group but not in the liraglutide-treated group. Akt phosphorylation at Ser473 was not affected by either treatment.

Phosphorylation at the Ser9 epitope of GSK-3β, which is the primary tau kinase, significantly increased

Table 2
Metabolic parameters of 6 months old MSG mice after 14-day treatment with palm-PrRP31 and liraglutide

Intervention	Body weight [g]	White adipose tissue [% body weight]	Glucose [mmol/l]	Insulin [ng/ml]	Leptin [ng/ml]
Saline	53.08 ± 2.22	6.37 ± 0.84	6.48 ± 0.42	1.53 ± 0.20	23.10 ± 3.85
Palm-PrRPP31	50.07 ± 1.68	4.91 ± 0.43	6.49 ± 0.32	1.57 ± 0.13	21.20 ± 2.62
liraglutide	48.23 ± 1.70	5.38 ± 0.67	5.63 ± 0.34	1.91 ± 0.27	18.16 ± 2.41

Data are mean ± SEM ($n = 10$ animals per group). Data were analyzed by one-way ANOVA, Bonferroni *post hoc* test.

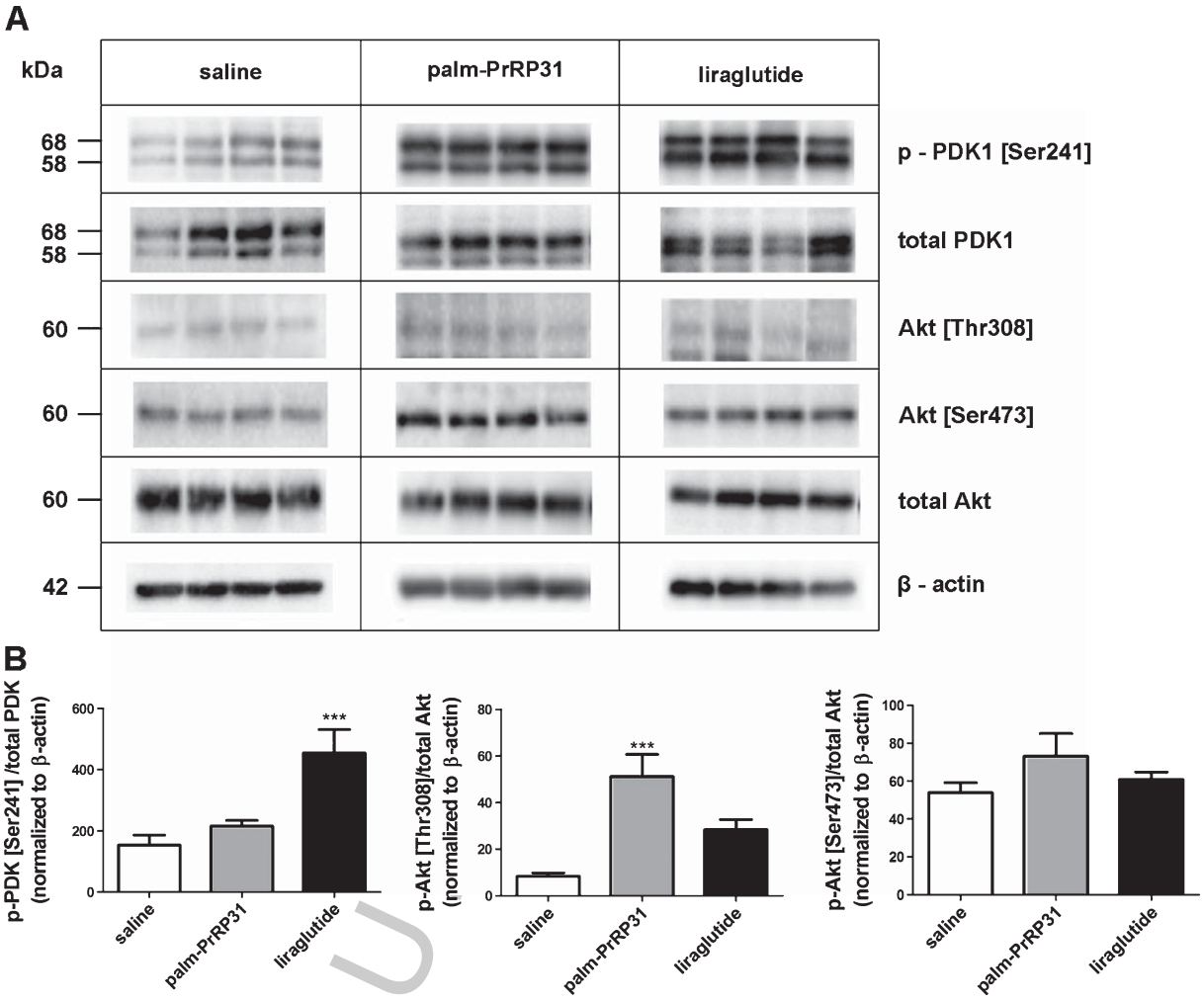

Fig. 4. Liraglutide and palm-PrRP31 enhance insulin signaling in the hippocampus. Insulin signaling cascade in hippocampi of MSG mice after palm-PrRP31 or liraglutide treatment. A) Western blots of the proteins involved in insulin signaling cascade using specific antibodies ($n = 10$ mice per group). B) Densitometric quantification of the western blots normalized to β-actin. Data are mean ± SEM. The data were analyzed by one-way ANOVA, Dunnett *post hoc* test. $^{*}p < 0.05$, $^{**}p < 0.001$, and $^{***}p < 0.001$ versus saline-treated group.

after palm-PrRP31 administration but not after liraglutide administration in the MSG-obese mice (Fig. 5).

The phosphorylation of two other potent tau kinases, ERK1/2 and JNK, was significantly lowered after both palm-PrRP31 and liraglutide administration in the hippocampi of the MSG-obese mice, as shown in Fig. 5.

Palm-PrRP31 and liraglutide reduced tau hyperphosphorylation in the hippocampi of MSG-obese mice

The phosphorylation of the hippocampal tau protein at the Thr212, Thr231, and Ser396 epitopes of the MSG-obese mice was affected by treatment with both palm-PrRP31 and liraglutide (Fig. 6). Both liraglutide and palm-PrRP31 treatment significantly decreased the hyperphosphorylation of the tau protein in these epitopes. The immunohistochemical analysis of the hippocampi confirmed these results. In the CA1 subfield of the hippocampus, the phosphorylation of the tau protein at Thr212 and at Ser202/T205 (the antibody AT8) decreased after palm-PrRP31 and liraglutide treatment compared with that of the control group (Fig. 7).

PrRP-R immunopositive cells are present in the hippocampus

PrRP-R immunopositive cells, which displayed small cell bodies and dendritic branches, were

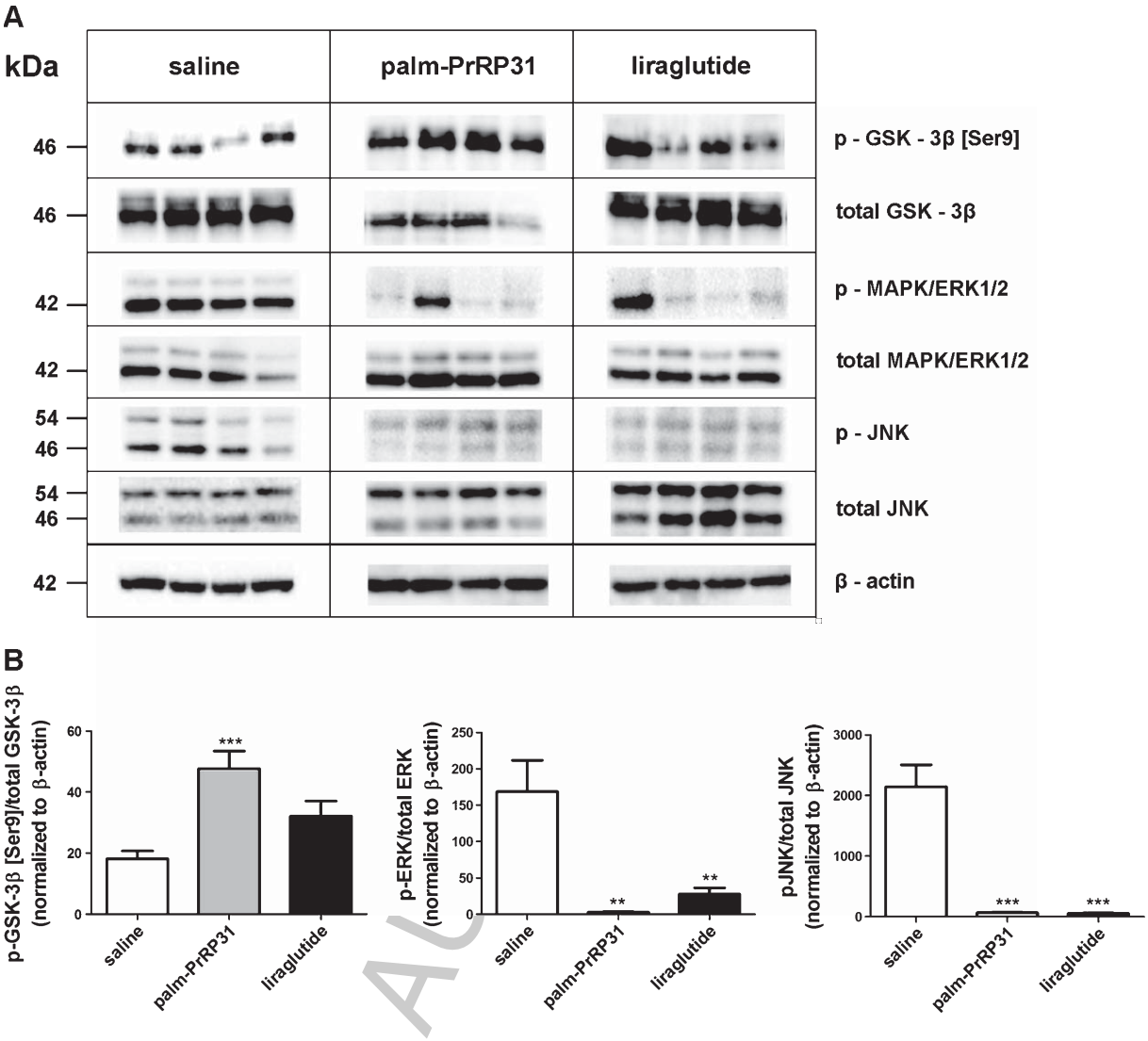

Fig. 5. Impact of liraglutide and palm-PrRP31 treatment on phosphorylation of hippocampal tau kinases GSK-3β, ERK1/2, and JNK. A) Western blots of the tau kinases phosphorylation using specific antibodies ($n = 10$ mice per group). B) Densitometric quantification of the western blots normalized to β-actin. Data are mean ± SEM. The data were analyzed by one-way ANOVA, Dunnett *post hoc* test. $^{*}p < 0.05$, $^{**}p < 0.001$, and $^{***}p < 0.001$ versus saline-treated group.

primarily detected in the stratum lacunosum-moleculare of the hippocampus (Fig. 8) and in the hilus proper of the dentate gyrus from control mice. In addition, several scattered PrRP-R cells were also detected in the stratum radiatum of the CA3 field of the hippocampus.

DISCUSSION

The primary results of this study revealed that treatment with palm-PrRP31, an analog of the anorexigenic neuropeptide PrRP that is active centrally after peripheral administration [34] and the T2DM drug liraglutide both had a central anorexigenic effect and decreased the phosphorylation of several tau kinases and of the tau protein in the hippocampus of 6-month-old pre-diabetic MSG-obese mice. Moreover, palm-PrRP31 and liraglutide abolished insulin signaling in the hippocampus in the MSG-obese mice.

MSG administration to mice or rats during the neonatal period led to "selective" lesions in the ARC [35, 36]; to pre-diabetic syndrome with mild hyperglycemia, hyperinsulinemia, and hyperleptinemia [36, 37]; and to decreased insulin sensitivity [38]. This pre-diabetic condition was also apparent in our MSG-obese mice at 2 and 6 months old.

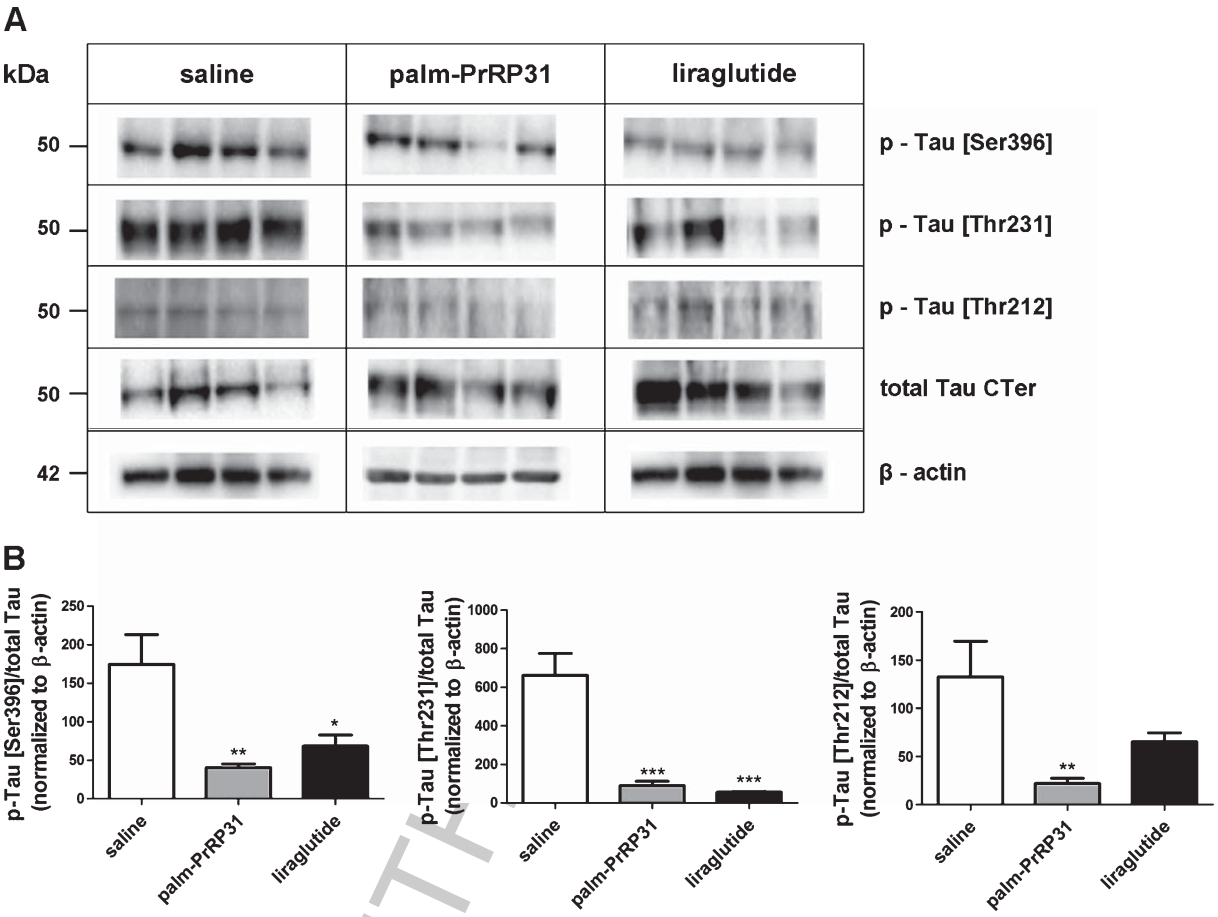

Fig. 6. Pathological hyperphosphorylation of tau protein is attenuated in hippocampi of MSG mice after liraglutide and palm-PrRP31 treatment. A) Western blots of tau phosphorylation on the epitopes Ser396, Thr231, and Thr212 ($n = 10$ mice per group). B) Densitometric quantification of western blots normalized to β-actin. Data are mean ± SEM. The data were analyzed by one-way ANOVA, Dunnett *post hoc* test. $^{*}p < 0.05$, $^{**}p < 0.001$, and $^{***}p < 0.001$ versus saline-treated group.

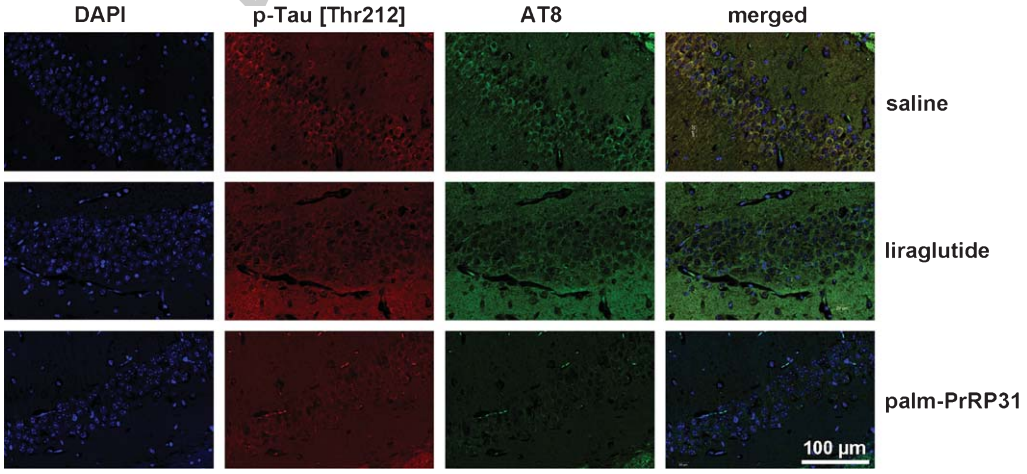

Fig. 7. Immunohistochemical staining of phosphorylated tau in hippocampi of MSG mice after liraglutide and palm-PrRP31 treatment. In hippocampal CA1 region from MSG mice, tau phosphorylation at Thr212 and at Ser202/Thr205 was detected after liraglutide or palm-PrRP31 treatment compared to saline-treated group. The nuclei were counterstained with DAPI (4′,6-diamidino-2-phenylindole).

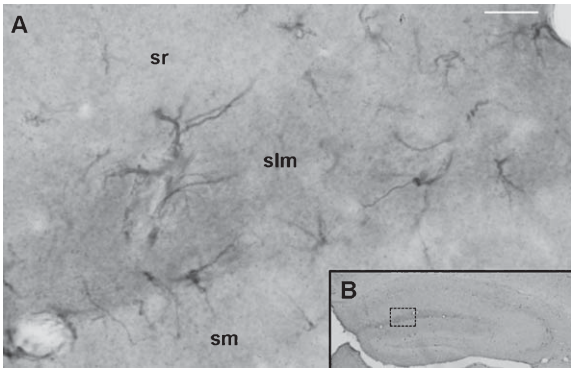

Fig. 8. The PrRP receptor immunopositive cells in the stratum lacunosum-moleculare (slm) of the control mice hippocampus. A) The detailed picture of PrRP receptor immunopositive cells in the stratum lacunosum-moleculare (slm) of the untreated control NMRI mice hippocampus. The white scale bar = 20 μm. B) The lower resolution picture of mice hippocampus with the denoted square area from which detailed pictures (A) was taken. slm, stratum lacunosum-moleculare; sm, stratum moleculare; sr stratum radiatum.

Although an age-related significant decrease in the phosphorylation of inhibitory Ser9 in GSK-3β, which augmented GSK-3β kinase activity, was obvious in controls but not in our MSG-obese mice, significantly enhanced phosphorylation of Thr231 and Ser396 of tau in the hippocampi was identified in the 6-month-old, but not in the 2-month-old, MSG-treated mice compared with controls. Tau hyperphosphorylation in pre-diabetic MSG-obese mice appears to be a progressive process similar to db/db mice with severe T2DM [9] and Zucker fa/fa rats [39]. Similarly, an increased phosphorylation at Ser396 in the neurofibrillary tangles and in dystrophic neurites has been found in the later stage of AD [40].

MSG-obese mice exhibit hyperleptinemia resulting from increased adiposity and from the loss of ARC neurons, which are the primary leptin targets [35, 36]. Recently, leptin resistance in the hippocampus was found to play a possible role in the characteristic changes associated with AD [41]. In contrast, leptin administration protected cortical and hippocampal cells from Aβ-induced expression of synaptic protein and tau hyperphosphorylation *in vitro* and *in vivo* [42].

Leptin controls PrRP production in the hypothalamus, and the anorexigenic effect of PrRP is synergistic with leptin [43]. Additionally, the present study demonstrated the presence of the PrRP receptor in the stratum lacunosum-moleculare of the CA1 subfield of the hippocampus and in the hilus of the dentate gyrus from control mice. These findings allowed rational assumption for the study of the palm-PrRP31 treatment also in obese MSG mice. Liraglutide was shown to cross the blood-brain barrier and to increase cAMP and neurogenesis in the mouse brain [44]. Learning and memory were restored after GLP-1 receptor (GLP-1R) gene transfer to the hippocampus in GLP-1R-deficient mice [45]. Although the central effect of liraglutide has recently been demonstrated to be only anorexigenic [19], liraglutide ameliorated hippocampal tau hyperphosphorylation in rats with STZ-induced severe T2DM in established DIO [46] and improved spatial memory and hippocampal neurogenesis in DIO mice [47, 48].

Moreover, different effects of diabetes on tau hyperphosphorylation have been identified in AD mouse models, in STZ-treated pR5 mice expressing P301L mutant tau [49], and in THY/Tau22 transgenic mice overexpressing human mutated tau with DIO [50]. STZ-induced diabetes exacerbated tau pathology in pR5 mice, whereas a detrimental effect of DIO on tau pathology in THY/Tau22 mice was related to obesity rather than to insulin resistance, whether peripheral or central. This study demonstrated that tau hyperphosphorylation could occur in the hippocampi of mice with obesity connected with pre-diabetes and that anorexigenic peptides with potent anti-obesity effects could attenuate this hypothetical tau hyperphosphorylation. Because the central effects of liraglutide have been proven exclusively anorexigenic and because palm-PrRP31 is an analog of a potent anorexigenic neuropeptide whose anti-diabetic effect has not yet been demonstrated, we conclude that the anorexigenic rather than anti-diabetic effects of both liraglutide and palm-PrRP31 mediated the decrease in tau phosphorylation in the hippocampi of the MSG-treated obese mice. In this study, we found that liraglutide and palm-PrRP31 attenuated the effects on tau hyperphosphorylation, although a 9-day treatment with both liraglutide and palm-PrRP31 did not affect the global utilization of glucose in the MSG-obese mice. In contrast, food intake significantly decreased after treatment with both substances.

In conclusion, 14-day peripheral administration of the anorexigenic lipopeptides, palm-PrRP31 and liraglutide, ameliorated hippocampal insulin signaling, decreased the activity of major tau kinases, and attenuated the pathological hyperphosphorylation of tau in MSG-obese mice, which are a model of obesity and pre-diabetes. These findings support the potential use of these analogs for the prevention and treatment of the tau hyperphosphorylation that is connected with obesity-related T2DM and describe, for the first time, the neuroprotective effect of PrRP.

ACKNOWLEDGMENTS

This study was supported by the Grant Agency of the Czech Republic No. P303/12/0576, and by the Academy of Sciences of the Czech Republic RVO: 61388963.

We gratefully acknowledge M. Blechová for synthesis of palm-PrRP31 analog, H. Vysušilová for excellent technical assistance, the laboratory of histology at Faculty of Medicine, Lille 2 university for preparing paraffin embedded slices, and Meryem Tardivel and IMPRT (Institut de Médecine Prédictive et de Recherche Thérapeutique, Lille) for access to the confocal microscopy platform.

Authors' disclosures available online (http://j-alz.com/manuscript-disclosures/14-3150).

SUPPLEMENTARY MATERIAL

The supplementary material is available in the electronic version of this article: http://dx.doi.org/10.3233/JAD-143150.

REFERENCES

[1] Martin L, Latypova X, Wilson CM, Magnaudeix A, Perrin ML, Yardin C, Terro F (2013) Tau protein kinases: Involvement in Alzheimer's disease. *Ageing Res Rev* **12**, 289-309.

[2] Buee L, Bussiere T, Buee-Scherrer V, Delacourte A, Hof PR (2000) Tau protein isoforms, phosphorylation and role in neurodegenerative disorders. *Brain Res Brain Res Rev* **33**, 95-130.

[3] Kolarova M, Garcia-Sierra F, Bartos A, Ricny J, Ripova D (2012) Structure and pathology of tau protein in Alzheimer disease. *Int J Alzheimers Dis* **2012**, 731526.

[4] Lee G, Leugers CJ (2012) Tau and tauopathies. *Prog Mol Biol Transl Sci* **107**, 263-293.

[5] Cavallini A, Brewerton S, Bell A, Sargent S, Glover S, Hardy C, Moore R, Calley J, Ramachandran D, Poidinger M, Karran E, Davies P, Hutton M, Szekeres P, Bose S (2013) An unbiased approach to identifying tau kinases that phosphorylate tau at sites associated with Alzheimer disease. *J Biol Chem* **288**, 23331-23347.

[6] Tenreiro S, Eckermann K, Outeiro TF (2014) Protein phosphorylation in neurodegeneration: Friend or foe? *Front Mol Neurosci* **7**, 42.

[7] Wang QM, Fiol CJ, DePaoli-Roach AA, Roach PJ (1994) Glycogen synthase kinase-3 beta is a dual specificity kinase differentially regulated by tyrosine and serine/threonine phosphorylation. *J Biol Chem* **269**, 14566-14574.

[8] Liu Y, Liu F, Grundke-Iqbal I, Iqbal K, Gong CX (2011) Deficient brain insulin signalling pathway in Alzheimer's disease and diabetes. *J Pathol* **225**, 54-62.

[9] Kim B, Backus C, Oh S, Hayes JM, Feldman EL (2009) Increased tau phosphorylation and cleavage in mouse models of type 1 and type 2 diabetes. *Endocrinology* **150**, 5294-5301.

[10] Ramos-Rodriguez JJ, Ortiz O, Jimenez-Palomares M, Kay KR, Berrocoso E, Murillo-Carretero MI, Perdomo G, Spires-Jones T, Cozar-Castellano I, Lechuga-Sancho AM, Garcia-Alloza M (2013) Differential central pathology and cognitive impairment in pre-diabetic and diabetic mice. *Psychoneuroendocrinology* **38**, 2462-2475.

[11] Jolivalt CG, Lee CA, Beiswenger KK, Smith JL, Orlov M, Torrance MA, Masliah E (2008) Defective insulin signaling pathway and increased glycogen synthase kinase-3 activity in the brain of diabetic mice: Parallels with Alzheimer's disease and correction by insulin. *J Neurosci Res* **86**, 3265-3274.

[12] Long-Smith CM, Manning S, McClean PL, Coakley MF, O'Halloran DJ, Holscher C, O'Neill C (2013) The diabetes drug liraglutide ameliorates aberrant insulin receptor localisation and signalling in parallel with decreasing both amyloid-beta plaque and glial pathology in a mouse model of Alzheimer's disease. *Neuromolecular Med* **15**, 102-114.

[13] McClean PL, Parthsarathy V, Faivre E, Hölscher C (2011) The diabetes drug liraglutide prevents degenerative processes in a mouse model of Alzheimer's disease. *J Neurosci* **31**, 6587-6594.

[14] Faivre E, Holscher C (2013) Neuroprotective effects of D-Ala(2)GIP on Alzheimer's disease biomarkers in an APP/PS1 mouse model. *Alzheimers Res Ther* **5**, 20.

[15] Li Y, Duffy KB, Ottinger MA, Ray B, Bailey JA, Holloway HW, Tweedie D, Perry T, Mattson MP, Kapogiannis D, Sambamurti K, Lahiri DK, Greig NH (2010) GLP-1 receptor stimulation reduces amyloid-beta peptide accumulation and cytotoxicity in cellular and animal models of Alzheimer's disease. *J Alzheimers Dis* **19**, 1205-1219.

[16] Yarchoan M, Arnold SE (2014) Repurposing diabetes drugs for brain insulin resistance in Alzheimer disease. *Diabetes* **63**, 2253-2261.

[17] Lannert H, Hoyer S (1998) Intracerebroventricular administration of streptozotocin causes long-term diminutions in learning and memory abilities and in cerebral energy metabolism in adult rats. *Behav Neurosci* **112**, 1199-1208.

[18] Li L, Zhang ZF, Holscher C, Gao C, Jiang YH, Liu YZ (2012) (Val(8)) glucagon-like peptide-1 prevents tau hyperphosphorylation, impairment of spatial learning and ultra-structural cellular damage induced by streptozotocin in rat brains. *Eur J Pharmacol* **674**, 280-286.

[19] Sisley S, Gutierrez-Aguilar R, Scott M, D'Alessio DA, Sandoval DA, Seeley RJ (2014) Neuronal GLP1R mediates liraglutide's anorectic but not glucose-lowering effect. *J Clin Invest* **124**, 2456-2463.

[20] Dodd GT, Luckman SM (2013) Physiological Roles of GPR10 and PrRP Signaling. *Front Endocrinol (Lausanne* **4**, 20.

[21] Ellacott K, Lawrence C, Rothwell N, Luckman S (2002) PRL-releasing peptide interacts with leptin to reduce food intake and body weight. *Endocrinology* **143**, 368-374.

[22] Greco SJ, Sarkar S, Johnston JM, Tezapsidis N (2009) Leptin regulates tau phosphorylation and amyloid through AMPK in neuronal cells. *Biochem Biophys Res Commun* **380**, 98-104.

[23] Greco SJ, Bryan KJ, Sarkar S, Zhu X, Smith MA, Ashford JW, Johnston JM, Tezapsidis N, Casadesus G (2010) Leptin reduces pathology and improves memory in a transgenic mouse model of Alzheimer's disease. *J Alzheimers Dis* **19**, 1155-1167.

[24] Fewlass DC, Noboa K, Pi-Sunyer FX, Johnston JM, Yan SD, Tezapsidis N (2004) Obesity-related leptin regulates Alzheimer's Abeta. *FASEB J* **18**, 1870-1878.

[25] Kamal A, Ramakers GM, Gispen WH, Biessels GJ (2013) Hyperinsulinemia in rats causes impairment of spatial memory and learning with defects in hippocampal synaptic

plasticity by involvement of postsynaptic mechanisms. *Exp Brain Res* **226**, 45-51.

[26] Li XL, Aou S, Oomura Y, Hori N, Fukunaga K, Hori T (2002) Impairment of long-term potentiation and spatial memory in leptin receptor-deficient rodents. *Neuroscience* **113**, 607-615.

[27] Djazayery A, Miller DS, Stock MJ (1979) Energy balances in obese mice. *Nutr Metab* **23**, 357-367.

[28] Maletínská L, Toma RS, Pirnik Z, Kiss A, Slaninová J, Haluzík M, Zelezná B (2006) Effect of cholecystokinin on feeding is attenuated in monosodium glutamate obese mice. *Regul Pept* **136**, 58-63.

[29] Remke H, Wilsdorf A, Müller F (1988) Development of hypothalamic obesity in growing rats. *Exp Pathol* **33**, 223-232.

[30] Blechová M, Nagelová V, Záková L, Demianová Z, Zelezná B, Maletínská L (2013) New analogs of the CART peptide with anorexigenic potency: The importance of individual disulfide bridges. *Peptides* **39**, 138-144.

[31] Maletínská L, Pýchová M, Holubová M, Blechová M, Demianová Z, Elbert T, Železná B (2012) Characterization of new stable ghrelin analogs with prolonged orexigenic potency. *J Pharmacol Exp Ther* **340**, 781-786.

[32] Sultan A, Nesslany F, Violet M, Begard S, Loyens A, Talahari S, Mansuroglu Z, Marzin D, Sergeant N, Humez S, Colin M, Bonnefoy E, Buee L, Galas MC (2011) Nuclear tau, a key player in neuronal DNA protection. *J Biol Chem* **286**, 4566-4575.

[33] Franklin K, Paxinos G (1997) *The mouse brain in stereotaxic coordinates*, New York: Academic Press.

[34] Maletinska L, Nagelova V, Ticha A, Spolcova A, Blechova M, Pirnik Z, Kunes J, Zelezna B (2013) Lipidized analogs of prolactin-releasing peptide reduce food intake in rodents after peripheral administration. *Biopolymers* **100**, 255-255.

[35] Takasaki Y (1978) Studies on brain lesion by administration of monosodium L-glutamate to mice. I. Brain lesions in infant mice caused by administration of monosodium L-glutamate. *Toxicology* **9**, 293-305.

[36] Matysková R, Maletínská L, Maixnerová J, Pirník Z, Kiss A, Železná B (2008) Comparison of the obesity phenotypes related to monosodium glutamate effect on arcuate nucleus and/or the high fat diet feeding in C57BL/6 and NMRI mice. *Physiol Res* **57**, 727-734.

[37] Cameron DP, Poon TK, Smith GC (1976) Effects of monosodium glutamate administration in the neonatal period on the diabetic syndrome in KK mice. *Diabetologia* **12**, 621-626.

[38] Lorden JF, Sims JS (1987) Monosodium L-glutamate lesions reduce susceptibility to hypoglycemic feeding and convulsions. *Behav Brain Res* **24**, 139-146.

[39] Spolcova A, Mikulaskova B, Krskova K, Gajdosechova L, Zorad S, Olszanecki R, Suski M, Bujak-Gizycka B, Zelezna B, Maletinska L (2014) Deficient hippocampal insulin signaling and augmented tau phosphorylation is related to obesity- and age-induced peripheral insulin resistance: A study in Zucker rats. *BMC Neurosci* **15**, 111.

[40] Su JH, Cummings BJ, Cotman CW (1994) Early phosphorylation of tau in Alzheimer's disease occurs at Ser-202 and is preferentially located within neurites. *Neuroreport* **5**, 2358-2362.

[41] Bonda DJ, Stone JG, Torres SL, Siedlak SL, Perry G, Kryscio R, Jicha G, Casadesus G, Smith MA, Zhu X, Lee HG (2014) Dysregulation of leptin signaling in Alzheimer disease: Evidence for neuronal leptin resistance. *J Neurochem* **128**, 162-172.

[42] Doherty GH, Beccano-Kelly D, Yan SD, Gunn-Moore FJ, Harvey J (2013) Leptin prevents hippocampal synaptic disruption and neuronal cell death induced by amyloid beta. *Neurobiol Aging* **34**, 226-237.

[43] Ellacott KL, Lawrence CB, Rothwell NJ, Luckman SM (2002) PRL-releasing peptide interacts with leptin to reduce food intake and body weight. *Endocrinology* **143**, 368-374.

[44] Hunter K, Holscher C (2012) Drugs developed to treat diabetes, liraglutide and lixisenatide, cross the blood brain barrier and enhance neurogenesis. *BMC Neurosci* **13**, 33.

[45] During MJ, Cao L, Zuzga DS, Francis JS, Fitzsimons HL, Jiao X, Bland RJ, Klugmann M, Banks WA, Drucker DJ, Haile CN (2003) Glucagon-like peptide-1 receptor is involved in learning and neuroprotection. *Nat Med* **9**, 1173-1179.

[46] Yang Y, Zhang J, Ma D, Zhang M, Hu S, Shao S, Gong CX (2013) Subcutaneous administration of liraglutide ameliorates Alzheimer-associated tau hyperphosphorylation in rats with type 2 diabetes. *J Alzheimers Dis* **37**, 637-648.

[47] Porter DW, Kerr BD, Flatt PR, Holscher C, Gault VA (2010) Four weeks administration of Liraglutide improves memory and learning as well as glycaemic control in mice with high fat dietary-induced obesity and insulin resistance. *Diabetes Obes Metab* **12**, 891-899.

[48] Lennox R, Porter DW, Flatt PR, Gault VA (2013) (Val(8))GLP-1-Glu-PAL: A GLP-1 agonist that improves hippocampal neurogenesis, glucose homeostasis, and beta-cell function in high-fat-fed mice. *ChemMedChem* **8**, 595-602.

[49] Ke YD, Delerue F, Gladbach A, Götz J, Ittner LM (2009) Experimental diabetes mellitus exacerbates tau pathology in a transgenic mouse model of Alzheimer's disease. *PLoS One* **4**, e7917.

[50] Leboucher A, Laurent C, Fernandez-Gomez FJ, Burnouf S, Troquier L, Eddarkaoui S, Demeyer D, Caillierez R, Zommer N, Vallez E, Bantubungi K, Breton C, Pigny P, Buée-Scherrer V, Staels B, Hamdane M, Tailleux A, Buée L, Blum D (2013) Detrimental effects of diet-induced obesity on τ pathology are independent of insulin resistance in τ transgenic mice. *Diabetes* **62**, 1681-1688.